Aus dem Institut für Klinische Biochemie und Pathobiochemie des Deutschen Diabetes-Zentrums der Heinrich-Heine-Universität Düsseldorf:

Direktor: Univ.-Prof. Dr. rer. nat. Hadi Al-Hasani

Impact of carbohydrate restriction on hepatic energy substrate metabolism in *Tbc1d4*-deficient mice

Dissertation

zur Erlangung des Grades eines Doktors der Medizin
der Medizinischen Fakultät der Heinrich-Heine-Universität Düsseldorf

vorgelegt von

Leonie Paula Förster

2026

Als Inauguraldissertation gedruckt mit Genehmigung der

Medizinischen Fakultät der Heinrich-Heine-Universität Düsseldorf

gez.:

Dekan: Prof. Dr. med. Nikolaj Klöcker

Erstgutachterin: PD Dr. rer. nat. Alexandra Chadt

Zweitgutachterin: Univ.-Prof. Dr. med. Maria Grandoch

Teile dieser Arbeit wurden veröffentlicht:

Kongressbeiträge:

Leonie Paula Förster, Anna K. Scheel, Hadi Al-Hasani, Alexandra Chadt. Diabetes Kongress (DDG), Berlin, Germany, 2024. **Protective effects of carbohydrate restriction on the liver of insulin resistant mice with a deficiency in *Tbc1d4*.** Diabetologie und Stoffwechsel 2024; 19(S 01): S86-S87, DOI: 10.1055/s-0044-1785407.

Summary

The RabGAP TBC1D4 is central to regulating glucose homeostasis and lipid metabolism in adipose tissue and skeletal muscle. Insulin-mediated translocation of GLUT4 to the plasma membrane facilitates glucose uptake. *Tbc1d4*-deficiency in mice reduces GLUT4 abundance and causes postprandial hyperglycemia and hyperinsulinemia. The loss-of-function mutation *TBC1D4* p.Arg684Ter, identified in Arctic populations such as the Greenlandic Inuit, is linked to postprandial hyperglycemia, hyperinsulinemia, and a novel subtype of type 2 diabetes (T2D) in homozygous carriers. Over the past decades, the incidence of T2D has markedly increased in this population. With a high allele frequency (4 % homozygous carriers in indigenous Inuit populations), the mutation is considered a possible evolutionary adaptation to the Arctic lifestyle of hunter-gatherer populations, where prolonged glucose clearance may have been advantageous under scarce carbohydrate intake and high physical activity. In contrast, the shift to a sedentary lifestyle and Westernized diet is a key factor in the rising T2D incidence. Our working group recently showed that moderate treadmill training overcomes genetically induced insulin resistance in *Tbc1d4*-knockout mice (D4KO). A follow-up study from our group further demonstrated that dietary carbohydrate restriction prevents postprandial hyperglycemia in these animals, presumably via an interplay of insulin-responsive tissues such as liver, skeletal muscle, and adipose tissue.

This study examined the impact of a Western, high-carbohydrate, low-protein diet (WD) versus a low-carbohydrate, high-protein diet (LCHP) on hepatic glucose and lipid metabolism in D4KO mice, as well as interactions between the liver and peripheral insulin-sensitive tissues. The results show that macronutrient ratios strongly influence metabolism: a WD promotes lipid turnover and hepatic triglyceride accumulation, whereas a LCHP diet protects glucose and lipid metabolism and prevents hepatic lipid accumulation. Insulin resistance in skeletal muscle and adipose tissue also alters hepatic gene and protein expression. These findings suggest that a LCHP diet could contribute to the prevention and treatment of T2D and associated liver complications in homozygous carriers of the p.Arg684Ter variant.

Zusammenfassung

Das RabGAP TBC1D4 spielt eine zentrale Rolle bei der Regulierung der Glukosehomöostase und des Fettstoffwechsels in Fettgewebe und Skelettmuskel. Die insulinvermittelte Translokation von GLUT4 zur Plasmamembran erleichtert die Glukoseaufnahme. Ein *Tbc1d4*-Mangel bei Mäusen reduziert die GLUT4-Menge und verursacht postprandiale Hyperglykämie und Hyperinsulinämie. Die Funktionsverlustmutation *TBC1D4* p.Arg684Ter, identifiziert in arktischen Populationen wie den grönländischen Inuit, steht in Zusammenhang mit postprandialer Hyperglykämie, Hyperinsulinämie und einem neuen Subtyp des Typ-2-Diabetes (T2D) bei homozygoten Trägern. In den letzten Jahrzehnten hat die T2D-Inzidenz in dieser Population deutlich zugenommen. Mit einer hohen Allelfrequenz (4 % homozygote Träger in indigenen Inuit-Populationen) gilt die Mutation als mögliche evolutionäre Anpassung an den arktischen Lebensstil von Jäger- und Sammlerpopulationen, bei dem eine verlängerte Glukose-Clearance unter knapper Kohlenhydratzufuhr und hoher körperlicher Aktivität vorteilhaft gewesen sein könnte. Im Gegensatz dazu trägt die Umstellung auf einen sitzenden Lebensstil und eine westliche Ernährung wesentlich zum Anstieg der T2D-Inzidenz bei. Unsere Arbeitsgruppe zeigte, dass moderates Laufbandtraining die genetisch bedingte Insulinresistenz bei *Tbc1d4*-Knockout-Mäusen (D4KO) überwindet. Eine Folgestudie unserer Gruppe belegte zudem, dass kohlenhydratarme Ernährung bei diesen Tieren postprandiale Hyperglykämie verhindert, vermutlich durch das Zusammenspiel insulinempfindlicher Gewebe wie Leber, Muskel und Fett.

Diese Studie untersuchte den Einfluss einer westlichen, kohlenhydratreichen, proteinarmen Diät (WD) gegenüber einer kohlenhydratarmen, proteinreichen Diät (LCHP) auf den hepatischen Glukose- und Lipidstoffwechsel in D4KO-Mäusen sowie die Wechselwirkungen zwischen Leber und peripheren insulinempfindlichen Geweben. Die Ergebnisse zeigen, dass das Makronährstoffverhältnis den Stoffwechsel stark beeinflusst: Eine WD fördert den Lipidumsatz und die Triglyceridakkumulation in der Leber, während eine LCHP-Diät den Glukose- und Lipidstoffwechsel schützt und die Lipidakkumulation verhindert. Zudem verändert die Insulinresistenz in Muskel und Fett die Gen- und Proteinexpression in der Leber. Diese Ergebnisse deuten darauf hin, dass eine LCHP-Diät zur Vorbeugung und Behandlung von T2D und damit verbundenen Leberkomplikationen bei homozygoten Trägern der p.Arg684Ter-Variante beitragen kann.

List of abbreviations

Acc1	Acetyl-CoA Carboxylase 1
aD4KO	Adipocyte-specific *Tbc1d4*-deficient mice
APS	Ammonium persulfate
AS160	TBC1D4
BCA	Bicinchoninic acid assay
CD36	Cluster of differentiation 36
cDNA	Complementary DNA
ChREBP	Carbohydrate responsive element binding protein
CON	Control Diet
Cpt1a	Carnitine Palmitoyltransferase 1a
Cpt2	Carnitine Palmitoyltransferase 2
Ct	Threshold cycle
D4KO	*Tbc1d4*-deficient mice
dNTP	Deoxyribonucleotide triphosphate
DNL	De novo lipogenesis
EDTA	Ethylenediaminetetraacetic acid
EGTA	Ethylene glycol-bis(β-aminoethyl ether)-*N*,*N*,*N*′,*N*′-tetraacetic acid
Elovl6	ELOVL Fatty Acid Elongase 6
EtOH	Ethanol
Fas	Fas Cell Surface Death Receptor
FASN	Fatty acid synthase
FoxO1	Forkhead box protein O1
GAP	GTPase-activating protein
GAPDH	Glyceraldehyde 3-phosphate dehydrogenase
GLUT4	Glucose transporter type 4
GSV	Glucose storage vesicle
GTP	Guanosine triphosphate
GYS2	Glycogen synthase 2
H3f3a	H3.3 Histone A
HCLP	High-carbohydrate low-protein diet
HDL	High density lipoprotein
HG	Hunter-gatherer
HGP	Hepatic glucose production
HSA	Human skeletal actin
IR	Insulin resistance
IRS	Insulin receptor substrates
LCHP	Low-carbohydrate high-protein diet
MASH	Metabolic dysfunction-associated steatohepatitis
MASL	Metabolic dysfunction-associated steatotic liver
mD4KO	Muscle-specific *Tbc1d4*-deficient mice
Me1	Malic enzyme 1
MgCl2	Magnesium chloride
MLX	Max-like protein X
Mlxipl	MLX Interacting Protein Like
mTORC1	Mammalian target of rapamycin complex 1
PBS	Phosphate-buffered saline
PCK1	Phosphoenolpyruvate Carboxykinase 1
PCK2	Phosphoenolpyruvate Carboxykinase 2

PI3K	Phosphatidylinositol-3-OH
PIP2	Phosphatidylinositol-4,5-bisphosphate
PIP3	Phosphatidylinositol-3,4,5-triphosphate
Pklr	Pyruvate kinase
Ppara	Peroxisome proliferator-activated receptor alpha
PUFA	Polyunsaturated fatty acids
Rab	Ras-related in brain
Rab-GAP	Rab-GTPase-activating protein
RT	Room temperature
RT-mix	Reverse transcriptase mix
RT-qPCR	Quantitative reverse transcription polymerase chain reaction
SDS-PAGE	Sodium dodecyl-sulfate polyacrylamide gel electrophoresis
Sirt1	Sirtuin 1
SLD	Steatotic liver disease
Srebf1	Sterol regulatory element-binding protein 1
Srebf2	Sterol regulatory element-binding protein 2
SREBP-1c	Sterol regulatory element-binding protein 1c
T1D	Type 1 Diabetes
T2D	Type 2 Diabetes
TG	Triglycerides
TBC1D1	TBC1 domain family member 1
TBC1D4	TBC1 domain family member 4
TEMED	Tetramethylethylenediamine
WD	Western Diet
WT	Wild Type

Table of contents

1 Introduction 1

1.1 Diabetes mellitus 1

1.2 Insulin resistance in peripheral tissues 2

1.3 MASLD and T2D 3

1.4 The impact of diet on T2D development 5

1.5 Insulin signaling in glucose and lipid metabolism 6

1.6 RabGAPs and their role in glucose and lipid metabolism 7

1.6.1 RabGAP variants in humans 9

1.6.2 RabGAP deficiency in mouse models 10

1.7 Aim of the thesis 14

2 Material and Methods 15

2.1 Material 15

2.1.1 Mouse strains 15

2.1.2 Mouse diets 15

2.1.3 Chemicals 16

2.1.4 Buffers and solutions 16

2.1.5 Reaction kits 17

2.1.6 Molecular weight size markers 18

2.1.7 Antibodies 18

2.1.8 Primers 19

2.1.9 Devices 20

2.1.10 Software 20

2.2 Methods 21

2.2.1 Molecular biological methods 21

2.2.1.1 RNA isolation from murine liver tissue 21

2.2.1.2 cDNA synthesis 21

2.2.1.3 (Quantitative Real-Time polymerase chain reaction (qPCR) 22

2.2.2 Biochemical methods 23

2.2.2.1 Preparation of protein lysates 23

2.2.2.2 Determination of total protein concentration 23

2.2.2.3 Sodium dodecyl sulfate polyacrylamide gel electrophoresis (SDS-PAGE) 24

2.2.2.4 Western blot and protein abundance analysis 25

2.2.2.5 Measurement of triglyceride levels in murine liver tissue 25

2.2.2.6 Statistical analysis 26

2.2.2.7 Use of AI-based language tools 26

3 Results 27

3.1 Impact of different dietary macronutrient ratios on hepatic energy substrate metabolism of Tbc1d4-deficient mice 27

3.1.1 Impact of dietary macronutrient ratios on expression levels of genes and protein abundance of key regulators of lipid metabolism in Tbc1d4-deficient mice 27

3.1.1.1 Impact of dietary macronutrient ratios on the expression levels of genes and abundance of proteins involved in lipid synthesis in the liver of Tbc1d4-deficient mice 27

3.1.1.2 Impact of diets on expression levels of genes involved in modification of fatty acids (desaturation and elongation) in the liver of Tbc1d4-deficient mice 30

3.1.1.3 Impact of diets on expression levels of genes involved in fatty acid oxidation in the liver of Tbc1d4-deficient mice 32

3.2 Hepatic triglyceride levels of Tbc1d4-deficient mice fed diets of differing macronutrient ratios 35

3.3 Impact of differing dietary macronutrient ratios on key regulators of glucose metabolism in the liver of Tbc1d4-deficient mice.....36

3.3.1 Impact of differing dietary macronutrient ratios on expression levels of genes and abundance of proteins regulating hepatic gluconeogenesis in the liver of Tbc1d4-deficient mice 36

3.3.2 Impact of differing dietary macronutrient ratios on expression levels of genes and protein abundance of regulators of glycolysis and lipogenesis in the liver of Tbc1d4-deficient mice.....38

3.3.3 Impact of differing dietary macronutrient ratios on mRNA expression levels of key factors regulating glycogen synthesis in the liver of Tbc1d4-deficient mice.....41

3.3.4 Impact of differing dietary macronutrient ratios on expression levels of genes involved in the regulation of insulin signaling in the liver of Tbc1d4-deficient mice.....41

4 Discussion 44

4.1 A LCHP diet exerts protective effects on hepatic lipid accumulation in Tbc1d4-deficiency ..45

4.2 A HCLP causes a shift from glucose to lipid metabolism in Tbc1d4-deficiency.....47

4.3 Downregulation of Pklr on a LCHP diet potentially improves glucose metabolism and hepatic lipid accumulation in peripheral tissues of Tbc1d4-deficient mice.....48

4.4 Reduced hepatic Elovl6 expression on a LCHP diet may indicate improved insulin sensitivity in peripheral tissues of Tbc1d4-deficient mice 48

4.5 Hepatic FASN abundance is influenced by a high-fat diet in Tbc1d4 deficiency 49

4.6 Potential link between GLUT4 dysfunction and Hepatic Mlxipl expression in aD4KO mice..49

4.7 Conclusion and outlook 51

5 References 53

6 Appendix 58

6.1 List of tables 58

6.2 List of figures 58

Danksagung.....59

1 Introduction

1.1 Diabetes mellitus

Diabetes mellitus is a chronic metabolic disease, characterized by elevated plasma glucose levels, and insulin resistance, insulin deficiency, or both [1, 2]. Several subtypes have been identified, the most common of which fall into two broad categories - type 1 and type 2 [2, 3]. In type 1 diabetes (T1D), an autoimmune process causes the destruction of pancreatic beta cells, leading to an absolute insulin deficiency. Most cases manifest in childhood and patients require lifelong insulin replacement therapy. Type 2 diabetes (T2D), in contrast, is characterized by peripheral insulin resistance, resulting in reduced insulin secretion. It can occur at any age, but classically manifests in adulthood [1, 2]. As there is still some insulin secretion left, most patients with T2D do not require insulin substitution [2, 4].

In 2021, 537 million cases of diabetes have been diagnosed in adults, of which over 90% can be attributed to T2D. The prevalence is increasing steadily and is expected to rise to 783 million by 2045 [5]. The etiology of T2D is multifactorial and has a strong genetic component. It is closely linked to the metabolic syndrome, which itself is defined by the presence of at least three out of the following criteria: abdominal obesity, hypertriglyceridemia, hypertension, low high-density lipoprotein (HDL) levels, and elevated fasting plasma glucose levels [6]. T2D is also strongly associated with a number of lifestyle factors, such as low physical activity, smoking, heavy alcohol use and air pollution [7]. Complications potentially arising from T2D include diabetic nephropathy, retinopathy, neuropathy, and cardiovascular diseases [2, 8]. T2D is thought to be largely preventable through changes in lifestyle, including dietary interventions [7, 9]. However, as eating behavior and the degree of metabolic improvements through exercise interventions are, to a substantial proportion, genetically determined, the identification of causal gene variants represents an important step in the development of personalized prevention and treatment options [10, 11].

1.2 Insulin resistance in peripheral tissues

T2D development is characterized by progressive insulin resistance (IR) in the liver, skeletal muscle, and adipose tissue, often developing over decades. IR is defined by the body's inability to respond to insulin, which results in impaired glucose uptake from the blood into the cells [12]. In the healthy state, an elevation of blood glucose levels triggers insulin production and secretion by pancreatic beta cells. In the insulin-resistant state, insulin-responsive target tissues do not respond adequately to the stimulus. Beta cells respond to the elevated blood glucose levels with sustained compensatory hyperinsulinemia which, in the long term, leads to exhaustion of the insulin-producing cells and, as a consequence, to a state of chronic hyperglycemia [13].

The liver plays a central role in glucose and lipid metabolism, with insulin being a critical regulator in both processes. The metabolism of glucose and lipids are intimately intertwined, with the body's capacity to switch between energy substrates dependent on substrate availability. In the fasting state, when insulin levels are low, fatty acids from adipose tissue reservoirs, mobilized through lipolysis, serve as the primary source of energy. Additionally, low insulin levels stimulate glycogenolysis and gluconeogenesis in the liver, maintaining plasma glucose levels within the desired range [14]. In the postprandial state, when glucose is readily available, insulin levels rise, suppressing hepatic glucose production. Insulin facilitates glucose uptake into muscle and adipose tissue, as well as hepatic glycogenesis and lipogenesis [15]. The ability of cells to switch between glucose and fatty acids for energy generation is defined as metabolic flexibility [16].

In the context of IR, despite elevated plasma glucose levels, insulin is unable to suppress hepatic glycogenolysis and gluconeogenesis, thereby further increasing hepatic glucose production (HGP). Concurrently, in insulin resistant adipose tissue, insulin is unable to inhibit lipolysis, resulting in the continuous release of non-esterified fatty acids into the circulation. This ultimately leads to ectopic lipid accumulation in muscle and liver tissue [17]. In skeletal muscle, IR is characterized by disturbed signaling downstream from the insulin receptor, ultimately leading to impaired GLUT4 translocation to the plasma membrane [18]. Consequently, the persistent surplus of fatty acids, in conjunction with the impaired glucose uptake, prompts the reliance of skeletal muscle on fat oxidation for energy. This imbalance impedes the appropriate

switching between fat and glucose utilization by tissues, a hallmark of metabolic inflexibility in states of insulin resistance [19].

IR is a common metabolic complication associated with obesity. Adipocyte hypertrophy and low-grade inflammation impair insulin's capacity to regulate lipolysis. Consequently, an excess of non-esterified fatty acids and pro-inflammatory mediators is released into the circulation, contributing to ectopic lipid deposition in the liver, where it exacerbates hepatic IR and disrupts glucose homeostasis. In skeletal muscle, the accumulation of lipid intermediates, such as diacylglycerols and ceramides, has been shown to interfere with insulin signaling, thereby limiting glucose uptake. Consequently, the metabolic and inflammatory alterations that accompany obesity lead to the development of insulin resistance across peripheral tissues [20].

1.3 MASLD and T2D

Steatotic liver disease (SLD) encompasses a wide range of liver diseases. Metabolic dysfunction–associated steatotic liver disease (MASLD) accounts for the most common chronic liver disease and is defined as liver steatosis together with at least one cardiometabolic risk factor. MASLD itself is a generic term for a set of liver conditions that are closely related to each other. This includes metabolic dysfunction-associated steatotic liver (MASL), which is defined as an ectopic accumulation of triglycerides (TGs) in the liver, called steatosis, metabolic dysfunction-associated steatohepatitis (MASH), which is characterized by inflammation and fibrosis in addition to liver steatosis, and cirrhosis. Cirrhosis is the most advanced form of MASLD and develops from progression of MASL and MASH [21].

Given the shared pathogenesis and risk factors, including alterations in lipid and glucose metabolism, IR and obesity, MASLD and T2D are closely related. In an IR state, increased lipolysis from dysfunctional adipose tissue and increased hepatic lipogenesis result in an excess of free fatty acids, which promote hepatic lipid accumulation and lipotoxicity. Furthermore, insulin is unable to suppress hepatic gluconeogenesis, resulting in glucose toxicity. This is characterized by a chronic elevation of plasma glucose levels and IR induced by glucose [22]. The prevalence of MASLD in T2D patients is estimated to be between 70 and 80% globally, and the coexistence of both conditions is associated with a more rapid progression of either.

Approximately half of the patients with both conditions will eventually develop MASH, and 3-5 percent of T2D patients will progress to cirrhotic liver disease [23]. The progression of MASLD, as well as the associated prevalence in patients with T2D, is illustrated in Figure 1.

Furthermore, glucotoxicity has been demonstrated to promote de novo lipogenesis (DNL), for example by activating Carbohydrate Responsive Element Binding Protein (ChREBP). In MASLD, DNL is significantly increased. A recent study has revealed that 15% of hepatic lipid accumulation in patients with MASLD can be attributed to dietary factors. Dietary carbohydrates represent a significant stimulus for DNL, as they activate hepatic lipogenic enzymes, including ChREBP, within the liver. It appears that an important contributor to the activation of DNL is excessive intake of industrial fructose, which is primarily cleared in the liver. Its metabolism is associated with an increase in lipogenesis and a corresponding accumulation of hepatic TGs [22, 24, 25].

The progression of MASL to MASH and fibrosis is significantly influenced by the effects of lipotoxicity and glucotoxicity. The accumulation of free fatty acids leads to the formation of toxic lipid intermediates, including diacylglycerols, ceramides, as well as oxidative stress and the formation of reactive oxygen species. The activation of inflammatory pathways causes the disease to progress [22, 23].

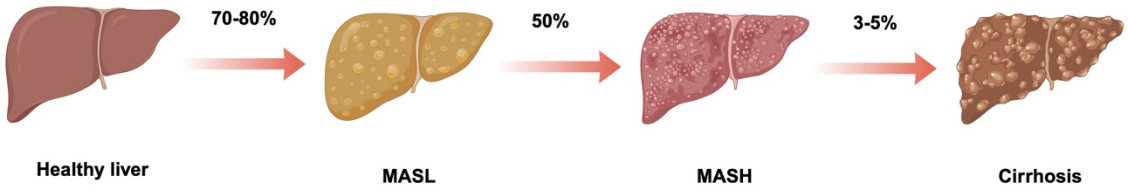


Figure 1: Progression and prevalence of MASLD.
Progression of metabolic dysfunction-associated liver disease (MASLD). 70-80% of patients with T2D develop metabolic dysfunction-associated steatotic liver (MASL), of which approximately 50% will further progress to metabolic dysfunction-associated steatohepatitis (MASH). 3-5% of patients will eventually develop liver cirrhosis [23]. Created with BioRender.com.

1.4 *The impact of diet on T2D development*

Obesity is closely associated with a Western lifestyle, which is typically characterized by smoking, excessive alcohol consumption, physical inactivity, and diets high in refined carbohydrates and calories [7]. Constant snacking and the consumption of foods with a high glycemic index and glycemic load contribute to sustained postprandial hyperglycemia and prolonged insulin secretion, leading to chronic hyperinsulinemia and an increased risk of developing T2D [26].

The Western diet (WD) is distinguished by a high intake of saturated and trans fats, carbohydrates, and ultra-processed food [27]. It is associated with an increased production of reactive oxygen species, IR, and low-grade inflammation [28]. The consumption of a WD has been linked to a number of chronic illnesses, including T2D, hypertension, cardiovascular diseases, and dementia [29].

The role of dietary carbohydrates in the development of T2D has been subject of considerable research interest, largely due to their effect on blood glucose levels. As glucose is primarily derived from carbohydrates, they exert a significant influence on postprandial blood glucose levels [30]. The recommended macronutrient ratios for energy uptake are 45 % to 65% for carbohydrates, 10% to 35% for protein, and 20% to 35% for fats [31].

A ketogenic diet is distinguished by a high fat content and a very low carbohydrate component, with the consumption of less than 50 grams of carbohydrates per day. This induces β-oxidation of fatty acids in skeletal muscle for energy production and in the liver, where excess acetyl-CoA is converted into ketone bodies for use by extrahepatic tissues. Ketogenic diets have been shown to have beneficial effects on weight reduction, particularly in individuals with T2D [32].

Further insights into the relationship between diet and metabolic health can be drawn from hunter-gatherer (HG) populations. They adhere to a so-called paleolithic diet, which is characterized by a low carbohydrate and high protein content compared to a WD, but with a similar fat content. Interestingly, in these populations and other non-westernized populations, civilization diseases occur relatively rarely, indicating a protective effect of those diets [26].

This aligns with the findings of a study conducted on diabetic Australian Aboriginal individuals. The study's results indicated that a temporary reversion to their traditional

HG lifestyle and diet led to significant improvements in fasting glucose, insulin, and TG levels. Consequently, this reversion resulted in an improvement in their risk of developing T2D [33].

In addition to dietary and lifestyle factors, genetics, and evolutionary adaptation also play an important role in the development of specific metabolic phenotypes. It has been observed that certain genetic variants have emerged in isolated populations, suggesting a genetic adaptation to climate and diet over time [34, 35]. Greenlandic Inuit, for instance, have developed a genetic adaptation to a diet rich in polyunsaturated fatty acids (PUFAs). These fatty acids have a considerable impact on size and weight, thereby influencing positive selection in this population [35]. One of the most notable examples underscoring the genetic contribution to T2D is the population of the Pima Indians in Arizona [34], whose exceptionally high prevalence of the disease, the highest reported worldwide, indicates a strong heritable component, with more than half of adults over 35 years of age being affected [36].

1.5 Insulin signaling in glucose and lipid metabolism

Glucose serves as the primary source of energy for the human body [37]. It can be derived directly from the breakdown of macronutrients or mobilized from energy stores through gluconeogenesis or glycogenolysis [38]. Despite fluctuations in substrate availability, blood glucose levels are maintained within a narrow range between 4 and 7 mM [39].

Insulin is the primary regulator of glucose homeostasis, controlling the uptake of glucose into cells. It is a peptide hormone that is produced and secreted by pancreatic beta cells in response to elevated blood glucose levels [24]. In the postprandial state, insulin exerts its effects on tissues involved in glucose metabolism, including skeletal muscle, adipose tissue, and the liver. These tissues possess insulin receptors on their cell surfaces, to which insulin binds. The primary mechanism through which insulin mediates its effects involves the phosphorylation of Insulin receptor substrates (IRS), which subsequently recruit phosphatidylinositol-3-OH (PI3K). This process leads to the formation of phosphatidylinositol-3,4,5-trisphosphate (PIP3) from phosphatidylinositol-4,5-bisphosphate (PIP2). PIP3 has been shown to induce the translocation of Akt to

the plasma membrane, where it undergoes activation and subsequently functions on other downstream substrates implicated in glucose and lipid metabolism [15].

In the liver, activation of Akt2 leads to decreased HGP and promotes glycogenesis, as well as the activation of lipogenesis. In a fed state, insulin mediates phosphorylation and thereby inactivation of the gluconeogenic transcription factor Forkhead box O1 (FoxO1) by Akt. This leads to inhibition of glycogenolysis and gluconeogenesis, while concurrently promoting the expression of Sterol regulatory element-binding protein 1c (SREBP-1c) to drive lipogenesis [17, 40]. SREBP1c is an important regulator of hepatic lipid and cholesterol metabolism that is activated by insulin. A key activator of SREBP-1c is mechanistic target of rapamycin complex 1 (mTORC1), which is a downstream target of Akt. Another regulator of hepatic lipid metabolism is ChREBP. In response to high insulin levels, hepatic glucose uptake is increased, activating the glucose-responsive transcription factor [40].

Insulin facilitates glucose uptake into skeletal muscle and adipose tissue by translocation of glucose transporter type 4 (GLUT4) from intracellular storage vesicles to the plasma membrane. Upon insulin binding, the insulin receptor undergoes autophosphorylation, initiating a signaling cascade involving IRS and subsequent activation of Akt2, the predominant isoform in insulin-responsive tissues [41].

Activated Akt2 phosphorylates AS160 (TBC1D4), a Rab-GTPase-activating protein (RabGAP), thereby inhibiting its activity. This enables the activation of Rab-GTPases, which regulate the translocation of GLUT4-containing vesicles to the plasma membrane, thereby increasing glucose uptake into the cell [42].

Although insulin is primarily recognized for its role in glucose metabolism, insulin signaling also plays a central role in lipid metabolism. Insulin exerts its influence on lipid metabolism primarily through the inhibition of lipolysis of TGs and the promotion of lipogenesis and glycogen synthesis [43].

1.6 RabGAPs and their role in glucose and lipid metabolism

The RabGAPs TBC1D1 and TBC1D4 are important regulators of GLUT4 vesicular trafficking in skeletal muscle and adipose tissue. Upon stimulation by insulin, AMPK, and exercise/ muscle contraction, they undergo phosphorylation and regulate the translocation of intracellular GLUT4 storage vesicles (GSV) to the plasma membrane,

thereby enabling the uptake of glucose from the bloodstream into the cells [44]. The structure of the RabGAPs comprises two amino-terminal phosphotyrosine-binding domains, in addition to a RabGAP domain [45].

As illustrated in Figure 2, following stimulation by insulin or muscle contraction, TBC1D4 and TBC1D1 undergo phosphorylation, which in turn regulates the recruitment of these proteins to GSV [46]. In this state, it is postulated that the Rab protein bound to the GSV is loaded with guanosine triphosphate (GTP), thereby enabling its translocation to the plasma membrane. In this way, the RabGAPs play a critical role in regulating insulin-stimulated glucose uptake from the blood into skeletal muscle and adipose tissue [47]. TBC1D1 is considered more critical for exercise endurance and physical capacity, whereas TBC1D4 is primarily involved in regulating insulin sensitivity in skeletal muscle and adipose tissue [48].

In vitro studies have identified several Ras-related in brain (Rab) proteins Rab2, Rab8, Rab10, Rab14, and Rab28 as substrates for the GAP domain of TBC1D4 and TBC1D1 [44, 49, 50].

Furthermore, both Rab-GAPs have been demonstrated to play a role in lipid metabolism. For instance, both TBC1D4 and TBC1D1 have been implicated in the cellular entry of fatty acids via fatty acid transporters through Rab proteins in muscle tissue [51, 52]. In the myocardium of mice, TBC1D4 has been demonstrated to regulate the insulin-stimulated translocation of the FA translocase cluster of differentiation 36 (FAT/CD36) to the plasma membrane via the Rab protein Rab8a [53]. These findings underscore the significance of Rab-GAPs in lipid metabolism, though further research is necessary to elucidate the full scope of their function.

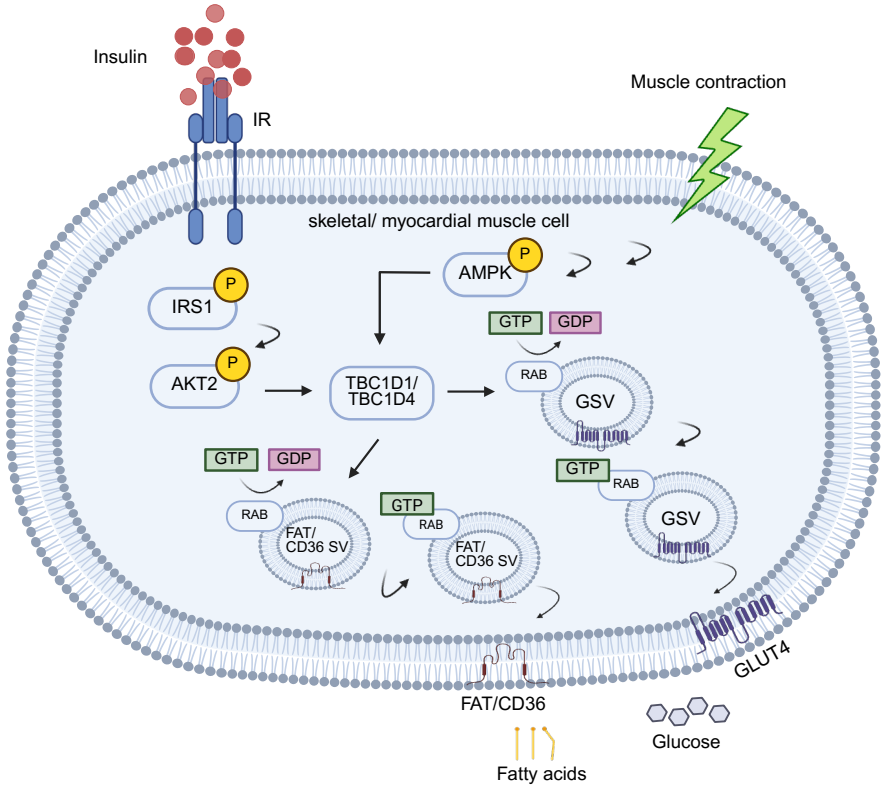


Figure 2: Involvement of RabGAPs in glucose and fatty acid uptake into skeletal/ myocardial muscle.
In response to insulin or muscle contraction, the insulin receptor undergoes conformational changes and phosphorylation, which in turn leads to phosphorylation of the IRS. This eventually leads to phosphorylation of Akt2. Phosphorylation of TBC1D4/ TBC1D1 enables the GTP-loaded GSV and FAT/CD36 SV to translocate to the plasma membrane, thereby facilitating their uptake. IRS = Insulin receptor substrate; Akt = Protein kinase B; AMPK = AMP-activated protein kinase; TBC1D4 = TBC1 family member 4; TBC1D1 = TBC1 family member 1; GSV = Glucose storage vesicle. SV = Storage Vesicle. Modification of an illustration from Dr. rer. nat. Pia M. Förster. Created with BioRender.com.

1.6.1 RabGAP variants in humans

A number of RabGAP variants have been identified in humans that are associated with obesity, insulin resistance, and T2D. For instance, a genetic variation in *TBC1D1*, *R125W*, has been linked to a predisposition to obesity in females [54]. Additionally, heterozygosity for a mutation in *TBC1D4*, *R363X*, has been associated with insulin resistance caused by reduced insulin stimulated GLUT4 cell membrane translocation [55].

Furthermore, a nonsense mutation in *TBC1D4*, *p.Arg684Ter*, was identified in Arctic populations, specifically in a Greenlandic Inuit population. Homozygosity for this variant resulted in a decrease in skeletal muscle GLUT4 abundance, which was associated with a reduction in insulin dependent GLUT4 translocation to the plasma membrane of skeletal muscle. This, in turn, was associated with postprandial

hyperglycemia, hyperinsulinemia, impaired glucose tolerance, and an increased susceptibility to developing T2DM. The mutation affects the long isoform of *TBC1D4*, which is primarily expressed in skeletal muscle and found on exon 11 [56]. It has been described that 4% of the Greenlandic Inuit population are homozygous carriers of the variant, which has been demonstrated to elevate the risk of developing T2D tenfold [57]. Additionally, by the age of 61, 80% of those carriers were found to have become diabetic [56]. It is postulated that the elevated prevalence of T2D in the Greenlandic Inuit population is at least partially attributable to an increasingly westernized lifestyle, including the consumption of processed, highly caloric food [58]. This contrasts with the traditional Arctic lifestyle, which is typified by a high level of physical activity, including hunting and fishing, and a diet rich in seafood [59].

A cross-sectional study of Greenlandic Inuit revealed that glycemic control improved following a dietary trial involving the traditional diet, which is marine food-based and low in carbohydrates, in comparison to a trial utilizing a WD, which is high in imported meats and carbohydrates. Moreover, the traditional diet was associated with weight loss and enhanced HDL levels [60]. These findings reinforce the significance of lifestyle and dietary habits in this population regarding the development of T2D.

1.6.2 RabGAP deficiency in mouse models

Global *Tbc1d4* knockout mice (D4KO) exhibit a phenotype comparable to that observed in human homozygous carriers of the *p.Arg684Ter* variant, including decreased fasting glucose levels and a reduction in insulin-mediated glucose uptake into skeletal muscle [56]. Moreover, similarly to humans, GLUT4 abundance in skeletal muscle was also decreased, leading to postprandial hyperglycemia and hyperinsulinemia [61]. Our group recently discovered that feeding of a traditional low-carbohydrate, high-protein (LCHP) diet was associated with enhanced insulin sensitivity in skeletal muscle of D4KO mice [62]. Fig. 3 demonstrates reduced plasma glucose levels after a 16 hour fast, followed by postprandial hyperglycemia on a control (CON) and high-carbohydrate, low-protein (HCLP) diet in D4KO and adipocyte-specific *Tbc1d4* knockout (aD4KO) mice, but not in muscle-specific *Tbc1d4* knockout (mD4KO) mice. Fig. 3.C, F, and I shows that on a LCHP diet, postprandial glucose levels remain low.

In addition to the reduced fasting plasma glucose levels observed in *Tbc1d4*-deficient mice, our study group also found that these findings were accompanied by elevated fasting plasma ketone bodies, particularly in mice fed a HCLP diet (Fig. 4.B and 4.H) [62]. This finding indicates that in *Tbc1d4*-deficiency, despite adequate glucose and fat availability, glucose utilization is inadequate leading to hepatic ketogenesis. These observations were exclusively discernible in D4KO mice and aD4KO mice, while they were absent in mD4KO mice (Fig. 4) [62]. The differences in blood glucose levels and ketone body concentrations between genotypes suggests a complex interplay between peripheral insulin sensitive tissues, as well as an involvement of the liver.

Furthermore, the two RabGAPs play an important role in lipid metabolism. Both TBC1D4 and TBC1D1 have been implicated in the cellular entry of fatty acids via fatty acid transporters through Rab proteins in muscle tissue [51, 52]. Additionally, previous studies from our group have shown that the combined absence of *Tbc1d1* and *Tbc1d4* in mice (D1/4KO) resulted in a shift in substrate utilization from glucose to fatty acids, as evidenced by a reduced respiratory quotient and increased fatty acid oxidation in isolated skeletal muscle [44].

Additionally, our group recently demonstrated that chronic moderate endurance exercise improved glucose and insulin tolerance in D4KO mice fed a high-fat diet. It also increased the expression of mitochondrial and browning markers in white adipose tissue and enhanced glucose clearance in brown and white adipose tissues, thereby compensating for the genetically induced peripheral insulin resistance in *Tbc1d4*-deficiency [63].

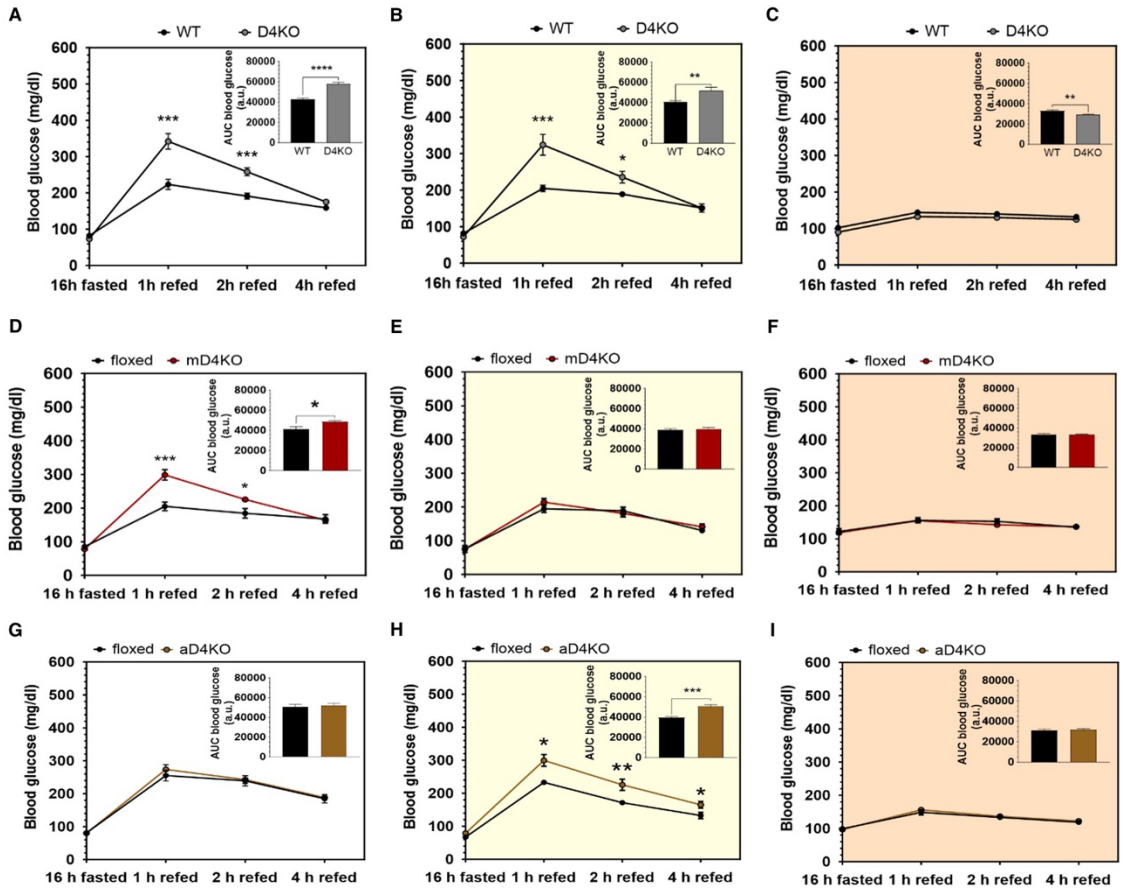


Figure 3: Impact of dietary macronutrient ratios on postprandial glycemia of *Tbc1d4*-deficient mice.
Determination of fasted and postprandial blood glucose concentrations and AUC (A.1–C.1) from *Tbc1d4*- (D4KO) mice and WT littermates aged 16–17 weeks subjected to a CON (A), HCLP (B) or LCHP (C) diet. Data are presented as mean ± SEM (n = 8-13). *p < 0.05, **p < 0.01, ***p < 0.001, AUC WT vs. D4KO (One-way ANOVA). Data by Dr. rer. nat. Anna K. Scheel, PhD Thesis, 2024.

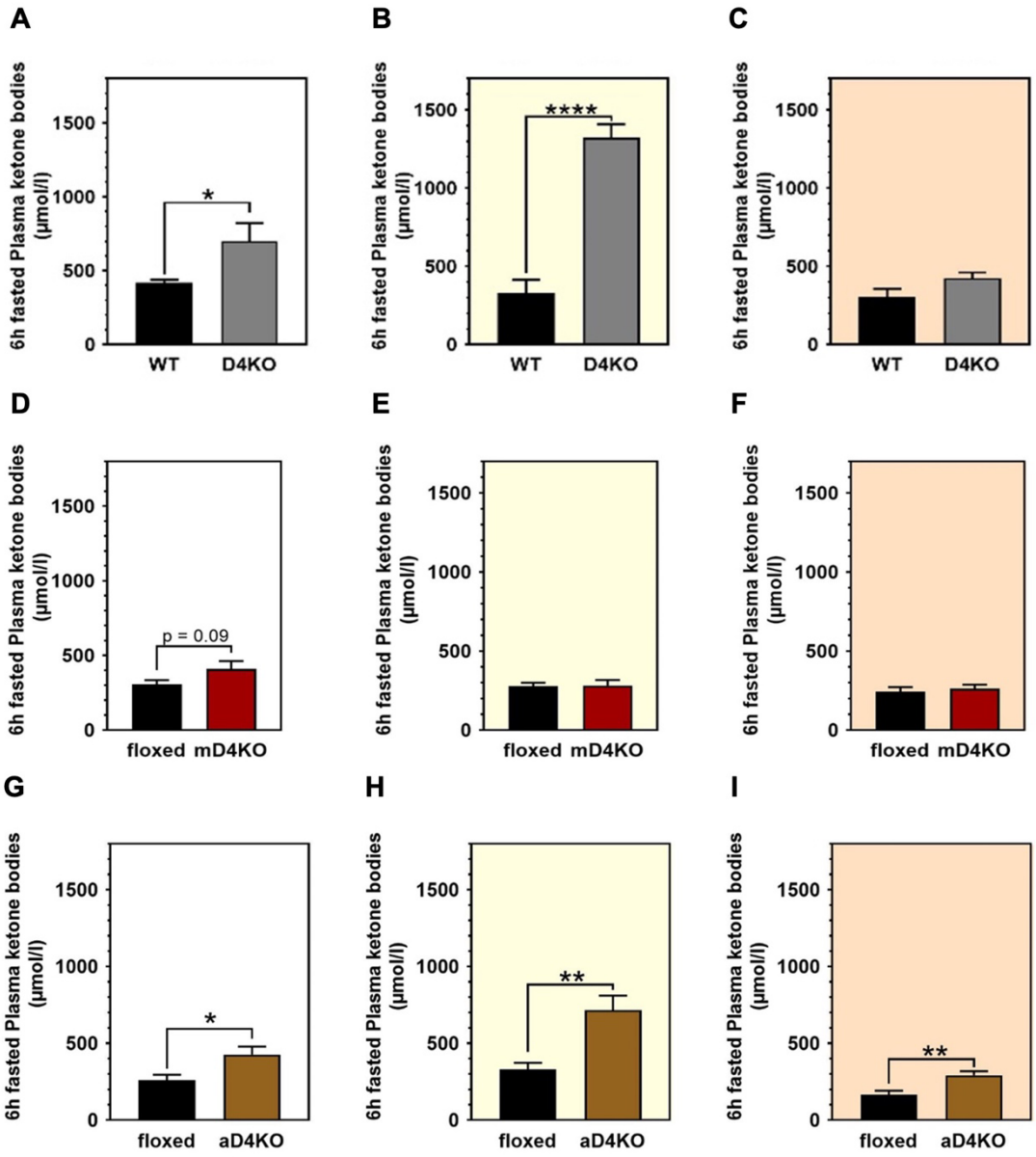


Figure 4: Impact of different macronutrient ratios on fasted plasma ketone bodies in mice with global (D4KO), skeletal muscle-specific (mD4KO) or adipocyte-specific (aD4KO) Tbc1d4-deficiency.
Determination of fasted plasma ketone bodies in D4KO (A-C), mD4KO (D-E) and aD4KO (G-I) mice fed a control diet (white), a HCLP diet (yellow), and a LCHP diet (orange). Data are presented as mean ± SEM (n = 7–9). *p<0.05, **p<0.01, ***p<0.001, ****p<0.0001 (Student's t-test). Data by Dr. rer. nat. Anna K. Scheel, PhD Thesis, 2024.

1.7 Aim of the thesis

The observation of improvements in the alterations associated with T2D in both humans [60] and mice [62] with *Tbc1d4*-deficiency, when fed a LCHP diet, indicates a beneficial effect of the diet on the risk of developing T2D. This thesis focuses on the effects of nutrition and tissue-specific *Tbc1d4*-deficiency on hepatic energy substrate metabolism, with a particular emphasis on the liver. It is of particular interest to ascertain whether a LCHP diet offers protection against alterations in hepatic lipid and glucose metabolism in mice deficient in *Tbc1d4*.

Furthermore, a cross-sectional study indicates that Greenlanders with T2D have a diminished probability of developing T2D-related liver complications when compared to a reference population [64]. The objective of this thesis is to elucidate the impact of nutrition on hepatic triglyceride accumulation in D4KO mice. Hepatic TG levels were measured in liver tissue samples of mice fed different macronutrient ratios and compared to their WT littermates. A particular focus is placed on the effects that a LCHP diet could have on hepatic TG levels and the potentially protective effects that the diet could have on the development of MASLD.

2 Material and Methods

2.1 Material

2.1.1 Mouse strains

This study utilized liver tissue samples from male C57BL/6J mice, sacrificed at 17-19 weeks of age. The samples were kindly provided by Dr. rer. nat. Anna K. Scheel, and the B6.Tbc1d4tm1-Tg(Adipoq- cre)1Evdr/J mouse line was originally provided by Prof. Dr. rer. nat. Jens W. Fischer and Prof. Dr. med. Maria Grandoch (University Hospital Düsseldorf, Germany). All animals were derived from experiments approved by the State Agency for Nature, Environment and Consumer Protection of North Rhine-Westphalia (LANUV, North Rhine-Westphalia, Germany) with the reference number 81-02.04.2019.A492, as previously described [62]. The following table (Table 1) provides a comprehensive listing of all mouse strains utilized in this study.

Table 1: Mouse strains

Strain	**Abbreviation**	**Supplier**
RCS.B6.SJL-Nob1.10B6/SJL-*Tbc1d4*-/-	D4KO	DDZ, Düsseldorf, Germany
B6.Tbc1d4tm1-Tg(ACTA1-cre)79Jme/J	mD4KO	DDZ, Düsseldorf, Germany
B6.*Tbc1d4*tm1-Tg(Adipoq-cre)1Evdr/J	aD4KO	DDZ, Düsseldorf, Germany

2.1.2 Mouse diets

Following a period of 3-4 weeks of weaning, the mice were subjected to either a control diet (CON), a HCLP, or a LCHP diet. The precise composition of the diets can be found in the following table (Table 2). The diets were provided by Research Diets (New Brunswick, NJ, USA).

Table 2: Composition of mouse diets

	CON (20092415)	**HCLP** (D20092413)	**LCHP** (D20092414)
	kcal %		
Carbohydrate	70	**40**	**5**
Fat	10	55	55
Protein	20	**5**	**40**
Kcal/gm	3.8	5.1	5.1

2.1.3 Chemicals

Throughout this study, the following chemicals were used:

Table 3: Chemicals

Chemical	**Supplier**
2-propanol (100%)	AppliChem, Darmstadt, Germany
5x HF Buffer	Mobidiag (Espo, Finland)
Acrylamid 4K Solution (37. 5:1, 30%)	AppliChem, Darmstadt, Germany
Agarose	Biozym Scientific, Oldendorf, Germany
Ammonium persulfate (APS)	Serva, Heidelberg, Germany
Chloroform	AppliChem, Darmstadt, Germany
Deoxynucleoside triphosphates (dNTPs)	Roche Diagnostics, Mannheim, Germany
Ethanol, absolute (EtOH)	Merck, Darmstadt, Germany
Ethylenediaminetetraacetic acid (EDTA)	Carl Roth, Karlsruhe, Germany
Ethylene-glycol-bis-(2-aminoethylether)-N,N,N',N'-tetraacetic acid (EGTA)	Carl Roth, Karlsruhe, Germany
HDGreenTM Plus DNA Stain	Intas Science Imaging Instruments, Göttingen, Germany
Hexanucleotide primer	Roche Diagnostics, Mannheim, Germany
Magnesium chloride ($MgCl_2$)	Promega, Madison WI, USA
Methanol	Carl Roth, Karlsruhe, Germany
Nuclease-free water	Promega, Madison WI, USA
Phosphatase inhibitor tablets (PhosSTOP)	Roche Diagnostics, Mannheim, Germany
Powdered milk	Carl Roth, Karlsruhe, Germany
Protease Inhibitor Cocktail tablets (complete)	Roche Diagnostics, Mannheim, Germany
Proteinase K	Carl Roth, Karlsruhe, Germany
Sodium chloride (NaCl)	Carl Roth, Karlsruhe, Germany
Tetramethylendiamine (TEMED)	Carl Roth, Karlsruhe, Germany
Tris	Carl Roth, Karlsruhe, Germany
Triton X-100	Sigma-Aldrich, St. Louis MO, USA
TRIzol Reagent	Thermo Scientific, Peqlab, Wilmington MA, USA
Tween 20	AppliChem, Darmstadt, Germany

2.1.4 Buffers and solutions

Throughout this study, the following buffers and solutions were used:

Table 4: Buffers and solutions

Buffer/ Solution	Composition/ Supplier
DNA isolation	
TAE buffer	40 mM Tris-HCl, 1 mM EDTA, 57.1 ml acetic acid, pH 8.0
TE buffer	10 mM Tris-HCl (pH 8.0), 1 mM EDTA (pH 8.0)
Protein and Western blot analysis	
Blocking solution	5 % powdered milk, TBS-Tween (1 x)
BSA standard (2 mg/ml)	Thermo Scientific, Perbio Science, Bonn, Germany
Electrophoresis buffer (10 x) 5 % powdered milk, TBS-Tween (1 x)	250 mM Tris, 1.92 mM glycine, 1 % SDS
Laemmli sample buffer (LSB) (4 x)	250 mM Tris, 10 mM EDTA, 20 % glycerol, 6 % DTT, 8 % SDS, 0.2 % bromophenol blue (pH 6.8)
Protein lysis buffer	20 mM Tris-HCl, 150 mM NaCl, 1 mM EDTA, 1 mM EGTA, 1 % Triton X-100 (pH 7.5) + freshly added 40 µl/ml protease inhibitor (cOmplete) and 100 µl/ml phosphatase inhibitor (PhosSTOP)
Separating gel buffer	1.5 M Tris, 0.4 % SDS (pH 8.8)
Stacking gel buffer	0.5 M Tris, 0.4 % SDS (pH 6.8)
TBS-Tween buffer (Tris-buffered- saline with Tween 20, TBS-T) (10 x)	100 mM Tris, 1.5 mM NaCl (+ 0.05 % Tween 20)
Transfer buffer (10 x)	250 mM Tris, 1.92 mM glycine (+ 20 % methanol)
Triglyceride analysis	
Phosphate buffered saline (PBS) without Mg^{2+} and Ca^{2+}	136.9 mM NaCl, 2.7 mM KCl, 1.5 mM KH_2PO_4, 8.06 mM Na_2HPO_4 x $2H_2O$ (pH = 7.4)

2.1.5 Reaction kits

Throughout this study, the following reactions kits were used:

Table 5: Reactions kits

Reaction kit	Application	Supplier
BCA Protein Assay Kit	Determination of protein concentration	Pierce, Rockford IL, USA
GoScript Reverse Transcription System	cDNA synthesis	Promega, Madison WI, USA
GoTaq qPCR Master Mix	qPCR	Promega, Madison WI, USA
Triglyceride-Glo Assay	Determination of TAGs in the liver	Promega, Madison WI, USA

Western Lightning ECL Enhanced	Western blot	PerkinElmer (Waltham, MA, USA)

2.1.6 Molecular weight size markers

Throughout this study, the following molecular weight size markers were used:

Table 6: Molecular weight size markers

Molecular weight size marker	**Supplier**
GeneRuler 100 bp DNA ladder	Thermo Scientific (Peqlab, Wilmington MA, USA)
Page Ruler	Thermo Scientific (Peqlab, Wilmington MA, USA)
Precision Plus Protein Dual Color Standards	BIO-RAD (Hercules, CA, USA)

2.1.7 Antibodies

Throughout this study, the following antibodies were used for Western blot analysis:

Table 7: Antibodies

Name of protein	**Host species**	**Supplier**	**Catalog number**	**Dilution in TBS-T**
Primary antibodies				
FASN	Rabbit	New England Biolabs (NEB)	C20G5	1:10,000 + 5% powdered milk diluted in 1x TBS-T
GAPDH	Rabbit	NEB	2118	1:2,000 + 5% powdered milk diluted in 1x TBS-T
GYS2	Rabbit	NEB	98348	1:10,000 + 5% powdered milk diluted in 1x TBS-T
PCK1	Rabbit polyclonal	Abcam	Ab87340	1:10,000 + 5% powdered milk diluted in 1x TBS-T
PCK2	Rabbit polyclonal	NEB	6924	1:10,000 + 5% powdered milk diluted in 1x TBS-T

Secondary antibodies				
Anti-rabbit IgG	Goat	Dianova, Hamburg, Germany - Jackson Immuno Research Laboratories	111-035-003	1:20,000 + 5 % powdered milk diluted in 1x TBS-T, 1:10,000 + 5 % powdered milk diluted in 1x TBS-T

2.1.8 Primers

Throughout this study, the following Primers were used for gene expression studies:

Table 8: SYBR-Green Primers

Gene symbol	Gene name	Primer sequence (5`→ 3`)
Acc1	Acetyl-CoA Carboxylase Alpha	Fwd: CC-GCC-AGC-CTG-AGT-TCT Rev: GGG-AGT-GCT-GGT-TTA-GCT-CC Rev: AGC-ACC-CGA-ACT-AGG-TGA-CA
Mlxipl	MLX Interacting Protein like	Fwd: AGG-TCC-CAG-GAT-CCG-AGC Rev: TCC-TCC-GTT-GCA-CAT-ACT-GAA
Cpt1a	Carnitine Palmitoyltransferase 1A	Fwd: ACT-CCG-CTC-GCT-CAT-TCC-G Rev: CAT-CTT-GAG-TGG-TGA-CCG-AGT
Cpt2	Carnitine Palmitoyltransferase 2	Fwd: GAA-TGA-CAG-CCA-GTT-CAG-GAA-G Rev: TGA-GAT-GTA-GCT-GGT-GTG-CT
Elovl6	Fatty Acid Elongase 5	Fwd: AGC-ACC-CGA-ACT-AGG-TGA-CA Rev: CCG-CAA-GGC-GTA-GTA-AGA-GT
Fas	Fas Cell Surface Death Receptor	Fwd: GTC-CTG-CCT-CTG-GTG-CTT-G Rev: TGG-TTG-ACA-GCA-AAA-TGG-GC
FoxO1	Forkhead Box O1	Fwd: CTA-AGA-GTT-AGT-GAG-CAG-GCT-ACA-T Rev: CAT-CCT-GCA-CAG-GAA-AGT-GC
H3f3a	Histone H3.3 i	Fwd: CAA-TTG-TGT-TCG-CAG-CCT-TC Rev: GAC-ACC-TCC-TTA-CTT-ACC-CCC
Me1	Malic Enzyme 1	Fwd: CGG-GAC-CCG-CAT-CTC-AAC-A Rev: TCC-ATT-AAC-AGG-AGA-TAC-CTG-TCG
Ppara	Peroxisome Proliferator-Activated Receptor Alpha	Fwd: GAG-TGC-AGC-CTC-AGC-CAA Rev: CAG-TGG-GGA-GAG-AGG-ACA-GA
Pck1	Phosphoenolpyruvate Carboxykinase 1	Fwd: GAG-ATG-TGG-CCA-GGA-TCG-AA Rev: ATA-CAT-GGT-GCG-GCC-TTT-CAT
Pklr	Pyruvate Kinase L/R	Fwd: CTG-TAA-AGA-TGC-AAC-ATG-CGA-TTG Rev: GGT-AGC-GAG-ACA-GAA-GCT-GA
Sirt1	Sirtuin 1	Fwd: TGA-CCG-ATG-GAC-TCC-TCA-CT Rev: ACA-AAA-GTA-TAT-GGA-CCT-ATC-CGC
Srebf1	Sterol Regulatory Element Binding Transcription Factor 1	Fwd: CTT-TTC-CTT-AAC-GTG-GGC-CT Rev: AGC-TGG-AGC-ATG-TCT-TCG-AT

Srebf2	Sterol Regulatory Element Binding Transcription Factor 2	Fwd: CTG-TCG-GGT-GTC-ATG-GGC Rev: GAC-AAA-CTG-TAG-CAT-CTC-GTC-G

2.1.9 Devices

Throughout this study, the following devices were used:

Table 9: Devices

Device	**Supplier**
Centrifuge 5415 C	Eppendorf (Hamburg, Germany)
Centrifuge 5424 R	Eppendorf (Hamburg, Germany)
ChemiDoc XRS+	Bio-Rad Laboratories (Munich, Germany)
GelDoc XR+	Bio-Rad Laboratories (Munich, Germany)
iMARK Microplate Reader	Bio-Rad Laboratories (Munich, Germany)
Mastercycler	Eppendorf, Hamburg, Germany
NanoDrop 2000	Thermo Scientific (Peqlab, Wilmington, MA, USA)
Quant Studio 7 Flex	Thermo Scientific (Peqlab, Wilmington, MA, USA)
Thermomixer Compact	Eppendorf (Hamburg, Germany)
TissueLyser II	Qiagen (Hilden, Germany)
Tecan infinite M200	Tecan (Crailsheim, Germany)

2.1.10 Software

Throughout this study, the following software were used:

Table 10: Software

Software	**Supplier**
GraphPad Prism 10	GraphPad Software Inc (San Diego, CA, USA)
Image Lab 6.0.1	Bio-Rad Laboratories (Munich, Germany)
NanoDrop 2000	Thermo Scientific (Peqlab, Wilmington, MA, USA)
ChatGPT (version GPT-5.3)	Open AI (San Francisco, CA, USA)
DeepL Write	DeepL GmbH, Cologne, Germany

2.2 Methods

2.2.1 Molecular biological methods

2.2.1.1 RNA isolation from murine liver tissue

Prior to gene expression studies, RNA was extracted from murine liver tissue samples. For the experiment, 40-50 g of ground tissue was utilized, to which 1 ml of TRIzol reagent (Table 3) and a steel ball were added to homogenize the sample in the Tissue Lyser II (Table 9) for 5 minutes at 25 Hz. Subsequently, the supernatant was incubated for 5 minutes at room temperature (RT) and transferred to a new 1.5-mL Eppendorf tube. Next, 200 µL of chloroform was added, and the samples were inverted for 15 seconds to ensure phase separation. Subsequently, the samples were incubated for 2-3 minutes at RT before centrifugation at 13.523 x g for 15 minutes at 4°C. Here, the samples were separated into three distinct phases: a lower red phase containing phenolchloroforme, an interphase, and a clear upper phase. The RNA-containing interphase was extracted and transferred to a new 1.5 mL tube. Then, 500 µL of 100% isopropanol was added and briefly inverted. Subsequently, the samples were incubated for 10 minutes at -20°C, after which they were centrifuged at a speed of 13.523 x g for 10 minutes at -4°C. The supernatant was discarded, and the remaining pellet was washed two times with 500 µL 75% ethanol, followed by centrifugation at 5.283 x g for 5 minutes at 4°C. After this, the samples were vortexed to loosen the pellet. The supernatant was discarded, and the remaining pellet was dried on a thermomixer (Table 9) for 30 minutes. The pellet was resuspended in 150 µL of RNase-free water and then incubated on a thermomixer for two minutes at 55°C. Finally, the samples were placed on ice for approximately one hour, after which the RNA concentration was determined using the NanoDrop 2000 spectrophotometer (Table 9) with UV absorbance measurements.

2.2.1.2 cDNA synthesis

To determine gene expression levels via quantitative polymerase chain reaction (qPCR), RNA was first transcribed into complementary DNA (cDNA), which was used as an amplification template. Initially, the RNA was diluted with RNase free water, using 2 µL and 8 µL, respectively. Subsequently, 1 µL of dNTPs and 2 µL of hexanucleotide primer (1:10 dilution) were added to each sample to obtain a final volume of 13 µL.

Subsequently, the samples were incubated in the Mastercycler (Table 9) for five minutes at 65°C (program cDNAPRE2), to allow primer annealing to the RNA template. Subsequently, the samples were incubated on ice for one minute, followed by 10 seconds of centrifugation. In the subsequent step, the reverse transcriptase mixture (RT-mix) was prepared, containing the following: per sample a total of 7 µL was prepared, comprising 4 µL of GoScript 5x reaction buffer, 2 µL of magnesium chloride (MgCl2), and 1 µL of GoScript Reverse Transcriptase. Finally, the RT-mix was added to the RNA mixture, and the samples were shortly centrifuged. The samples, with a final volume of 20 µL, were placed in the Mastercycler for the cDNA synthesis, program designated as cDNAPRO. During the course of the program, the samples were subjected to a series of temperature-dependent processes, including annealing for 5 minutes at 25°C, for primers bind to their complementary DNA sequence. Next, cDNA synthesis occurs during the elongation step for 60 minutes at 45°C. Finally, enzyme inactivation for 15 minutes at 70°C terminates the activity of the reverse transcriptase after successful synthesis of the cDNA strand. Subsequently, the samples were maintained in an infinite hold at 4°C. The cDNA was then diluted with DNase-free water in a 1:40 ratio and stored at a temperature of -20°C, while the RNA was stored at a temperature of -80°C, until further use.

2.2.1.3 (Quantitative Real-Time polymerase chain reaction (qPCR)

Quantitative real-time polymerase chain reaction (RT-qPCR) was employed to quantify the expression levels of genes of interest (Table 8).

For each experiment, a master mix was prepared, containing 5 µL of 2x GoTaq qPCR Master Mix (Table 5), 0.5 µL of forward primer, 0.5 µL of reverse primer (each working solution), and 4 µL of cDNA (1:40 dilution) to yield a total volume of 10 µL. This solution was pipetted as triplicates into a 384-well plate. Furthermore, 20 µL of Reference Dye CXR (Table 5) were added to 1 mL of 2x GoTaq qPCR Master Mix.

During qPCR, the samples are subjected to the following processes: a hot start 2 minutes at 95°C, to ensure the activation of the DNA polymerase; a denaturation step of 15 seconds at the same temperature, which is repeated 40 times to separate the double-stranded DNA into single-stranded DNA. Subsequently, annealing occurs at

60°C. In the final step, the process of dissociation occurs at temperatures between 60 and 95°C.

The results were analyzed using the GraphPad Prism 10 software (Table 10). The relative gene expression levels were normalized to the housekeeping gene H3.3 Histone A (*H3f3a*) using the ΔΔCt method, which was employed for the analysis and comparison of the data.

2.2.2 Biochemical methods

2.2.2.1 Preparation of protein lysates

Protein lysates were prepared using 40-50 g of ground frozen murine liver tissue. Subsequently, a steel ball and 600 µL of protein lysis buffer (Table 4) were added to a 2mL Safe-Lock Tube, which was then homogenized in the Tissue Lyser II (Table 9) for 5 minutes at 25 Hz. The homogenized tissue was then transferred to a new 1.5-mL Eppendorf tube and centrifuged at 15.871 x g for 10 minutes at 4°C. Finally, the supernatant was transferred to a new 1.5mL Eppendorf tube, leaving the insoluble debris. Furthermore, a 1:40 dilution of the lysate with MQ water was prepared for the subsequent determination of protein concentration. The remaining lysate was stored at -80°C for later use.

2.2.2.2 Determination of total protein concentration

Determination of total protein concentration was accomplished through the implementation of a bicinchoninic acid (BCA) assay, using the BCA Protein Assay Kit (Table 5) according to the manufacturer's instructions. This assay is dependent upon the capacity of proteins to reduce Cu^{2+} to Cu^{+} in an alkaline milieu. The reduced Cu^{2+} then reacts with the bicinchoninic acid, forming a purple-colored complex. The intensity of the color produced is proportional to the amount of protein present in the solution [65].

20 µL of the diluted protein lysates were pipetted as duplicates onto a 96-well plate together with a standard series, as detailed in Table 11. A reagent mixture was prepared containing solution A with bicinchoninic acid and solution B with copper

sulfate from the Protein Assay Kit in a 50:1 ratio. 200 µL of this reagent mix were added to the wells, followed by a 30-minute incubation of the plate at 37°C. Subsequently, the plate was transferred to the iMARK Microplate Reader (Table 9) for the measurement of protein concentration at a wavelength of 562 nm to determine protein concentration.

2.2.2.3 Sodium dodecyl sulfate polyacrylamide gel electrophoresis (SDS-PAGE)

Proteins were separated electrophoretically by sodium dodecyl sulfate-polyacrylamide gel electrophoresis (SDS-PAGE). In the initial phase of this technique, the proteins are denatured to impart a negative charge, utilizing SDS. Subsequently, the proteins are separated by applying an electrical current, which facilitates their migration to the electrodes through the polyacrylamide gel. The rate of migration of proteins through the gel is dependent upon their molecular weight. Smaller proteins migrate at a faster rate than larger proteins [66].

The protein lysates were diluted with 4x Laemmli sample buffer (Table 4) and MQ water. After dilution, the samples were boiled for 5 minutes at 95°C to ensure complete denaturation of the proteins, allowing for accurate size-based separation. Subsequently, the 20 µL of the protein samples were loaded into the wells of a 10% SDS gel (Table 11). Additionally, a protein marker (ladder) was included in one well to estimate the molecular weight of each protein. In conducting the experiments, 5 µL of Precision Plus Protein Dual Color Standards or Page ruler (Table 6) was employed, contingent upon the molecular weight of the protein of interest.

Following the loading of the gels, they were placed into an electrophoresis chamber, which was filled with 1x electrophoresis buffer (Table 4).

In the initial phase of the electrophoresis, a lower voltage of 50-70 V was applied for approximately 15 minutes for the samples to enter and align in the stacking gel. The electrophoresis was conducted for another 30-45 minutes at 150 V for protein separation.

Table 11: Composition of the SDS gel

Reagent	**Separating gel 10% (in ml)**	**Stacking gel (in ml)**

ddH2O	3.66	1.83
Separating or stacking gel buffer	2.34	780
Acrylamide (30%)	3	390
Ammonium persulfate (APS)	18	6
Tetramethyletyhlenediamine (TEMED)	9	3

2.2.2.4 Western blot and protein abundance analysis

The previously separated proteins were transferred to a nitrocellulose membrane. To transfer the proteins from the gel to the membrane, the gel was placed on the nitrocellulose membrane. Filter papers and a sponge pad were placed on each side, and the combination was placed in a transfer chamber filled with transfer buffer and a current was applied between the electrodes. The transfer was conducted for a period of 2 hours at a current of 0.2A.

Following the successful transfer, the membrane was incubated in 5% milk at room temperature to block any unspecific protein-binding sites. After one hour, the membrane was incubated with the primary antibody (Table 7) over night. Given the use of proteins of varying molecular weights, the membrane was divided into three sections, allowing for the identification of three distinct proteins with a single membrane.

Following an overnight incubation period, the membrane was subjected to a 30-minute wash with TBS-T (Table 4) on a seesaw. Subsequently, the membrane was incubated with the second antibody (Table 7) for an additional hour on a seesaw at room temperature. Subsequently, the membrane was washed again for a 30-minute period.

In the next step, the protein abundance was measured using either Western Lightning ECL Pro or Ultra solution (Table 5) and detected via the Chemidoc (Table 9). Subsequently, the Image Lab software (Table 10) was used for quantification of protein abundance.

2.2.2.5 Measurement of triglyceride levels in murine liver tissue

TG levels were measured using the Promega Triglyceride-Glo Assay (Table 5) according to the manufacturer’s instructions.

For the assay, 10 mg of frozen liver tissue was combined with 500 µL of phosphate-buffered saline (PBS) (Table 4) and a steel ball in a 2 mL Eppendorf tube. Subsequently, the samples were homogenized in the Tissue Lyser II (Table 9) for 5 minutes at 25 Hz. The samples were then diluted with glycerol lysis solution at a 1:50 ratio. The remaining homogenized tissue was transferred into a new 1.5 mL Eppendorf tube and stored at -80°C for subsequent analysis. A glycerol standard series was prepared using 2 µL of the glycerol standard (20 µM) and 248 µL of glycerol lysis solution. This was further diluted to generate seven standards and a blank, each containing 240 µL. The standard series can be utilized for two plates. Subsequently, 25 µL of diluted samples, standard, and background control were added to a 96-well plate, briefly vortexed, and incubated for 30 minutes at 37°C. Following the incubation, 50 µL of glycerol detection reagent was added to each well, and the plates were placed on a plate shaker for 30 to 60 seconds at 500 rpm. Following an additional hour of incubation at room temperature, the plates were transferred to the Tecan Infinite M200 (Table 9) for luminescence measurement. The data were analyzed using GraphPad Prism 10 (Table 10).

2.2.2.6 Statistical analysis

All data presented in this thesis are expressed as mean ± standard error of the mean (SEM). The sample numbers (n) used for each experiment are illustrated in the figure legends and ranged from 6-9 for all experiments. A two-way ANOVA was used to determine statistically significant differences between groups with Bonferroni correction. P-values of < 0.05 were considered statistically significant and are indicated in the figure legends. The statistical analysis and graphical illustration were conducted using GraphPad Prism 10 software.

2.2.2.7 Use of AI-based language tools

Language editing and phrasing assistance was provided using ChatGPT (Table 10) and DeepL Write (Table 10). All scientific content, data interpretation, analyses, and conclusions were solely developed by the author, who takes full responsibility. The use of these tools was strictly limited to language refinement and did not contribute to the scientific content or interpretation.

3 Results

3.1 Impact of different dietary macronutrient ratios on hepatic energy substrate metabolism of Tbc1d4-deficient mice

TBC1D4 is an important regulator of glucose and lipid metabolism [51]. Our research group previously demonstrated that D4KO and aD4KO mice fed a HCLP diet exhibited elevated plasma ketone bodies and correspondingly reduced fasting plasma glucose levels. However, these effects were reversed when the mice were placed on a LCHP diet [62]. Given that ketogenesis occurs in the liver [67], the objective of this study is to further elucidate the involvement of the liver in whole-body glycemia in *Tbc1d4*-deficient mice. Gene expression studies and protein abundance analyses of key regulators of lipid and glucose metabolism were conducted in liver tissue from D4KO, mD4KO, and aD4KO mice subjected to a CON, a HCLP, and a LCHP diet.

3.1.1 Impact of dietary macronutrient ratios on expression levels of genes and protein abundance of key regulators of lipid metabolism in Tbc1d4-deficient mice

To determine the impact that different dietary macronutrient ratios have on lipid metabolism of *Tbc1d4*-deficient mice, studies were conducted at both gene and protein levels.

3.1.1.1 Impact of dietary macronutrient ratios on the expression levels of genes and abundance of proteins involved in lipid synthesis in the liver of Tbc1d4-deficient mice

In this study, the expression levels of genes involved in lipid synthesis were measured in liver samples of *Tbc1d4*-deficient mice using qPCR (2.2.1.3). Additionally, the abundance of a key protein regulator of lipid synthesis was assessed by Western blotting (2.2.2.4). This evaluation examined changes at both the transcriptional and protein levels to identify where the most pronounced effects occur.

Acetyl-CoA Carboxylase Alpha (*Acc1*) encodes for a protein that catalyzes the rate-limiting step of fatty acid synthesis [68].

In control animals, hepatic *Acc1* expression levels were significantly increased on a HCLP diet compared to the CON diet (Fig. 5.A–C). In both mD4KO and aD4KO mice,

Acc1 expression levels were significantly increased on the HCLP compared to the CON or LCHP diets (Fig. 5.B and C). Additionally, in these genotypes, expression levels on the LCHP diet were significantly lower than those observed with CON feeding. *Acc1* expression levels were significantly increased in D4KO mice on the LCHP diet compared to the CON diet (Fig. 5.A). There were no statistically significant differences in *Acc1* expression levels between genotypes within the same dietary group.

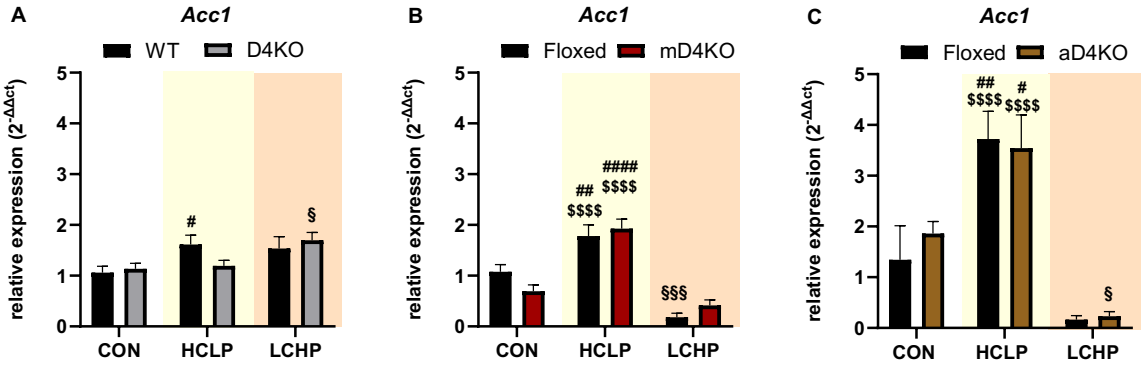


Figure 5: Gene expression levels of *Acc1* in the liver of global and tissue-specific D4KO mice.
Relative mRNA expression of Acetyl-CoA Carboxylase Alpha (*Acc1*) in D4KO (**A**), mD4KO (**B**), and aD4KO (**C**) mice and their WT/ floxed littermates subjected to a CON, HCLP or LCHP diet (n=6-9). Gene expression was normalized to the housekeeping gene *H3f3a*. Data shown represent mean ± SEM. Two-way ANOVA with Bonferroni-correction was used for statistical analysis. #p <0.05, ##p <0.01, ####p <0.0001, CON vs. HCLP. §p <0.05, §§§ <0.001, CON vs. LCHP. $$$$p <0.0001, HCLP vs. LCHP.

Sterol Regulatory Element Binding Transcription Factor 1 (*Srebf1*) is a transcription factor that regulates the expression of genes involved in the synthesis of lipids. It has been demonstrated that Sterol Regulatory Element Binding Transcription Factor 2 (*Srebf2*) regulates genes involved in the biosynthesis of cholesterol [69].

In control animals, hepatic *Srebf1* expression levels did not differ significantly among dietary conditions (Fig. 6.A–C). However, in D4KO mice, *Srebf1* expression levels were significantly higher on the LCHP diet than on the HCLP diet (Fig. 6.A). No significant dietary effects were observed in mD4KO or aD4KO mice (Fig. 6.B and C). There were no statistically significant differences in *Srebf1* expression levels between genotypes within the same dietary group.

As illustrated in Fig. 6.D, *Srebf2* expression levels were elevated in WT mice on HCLP and LCHP dietary groups relative to the CON group. No significant dietary effects were observed in mD4KO or aD4KO mice (Fig. 6.E and F). There were no statistically

significant differences in *Srebf2* expression levels between genotypes within the same dietary group.

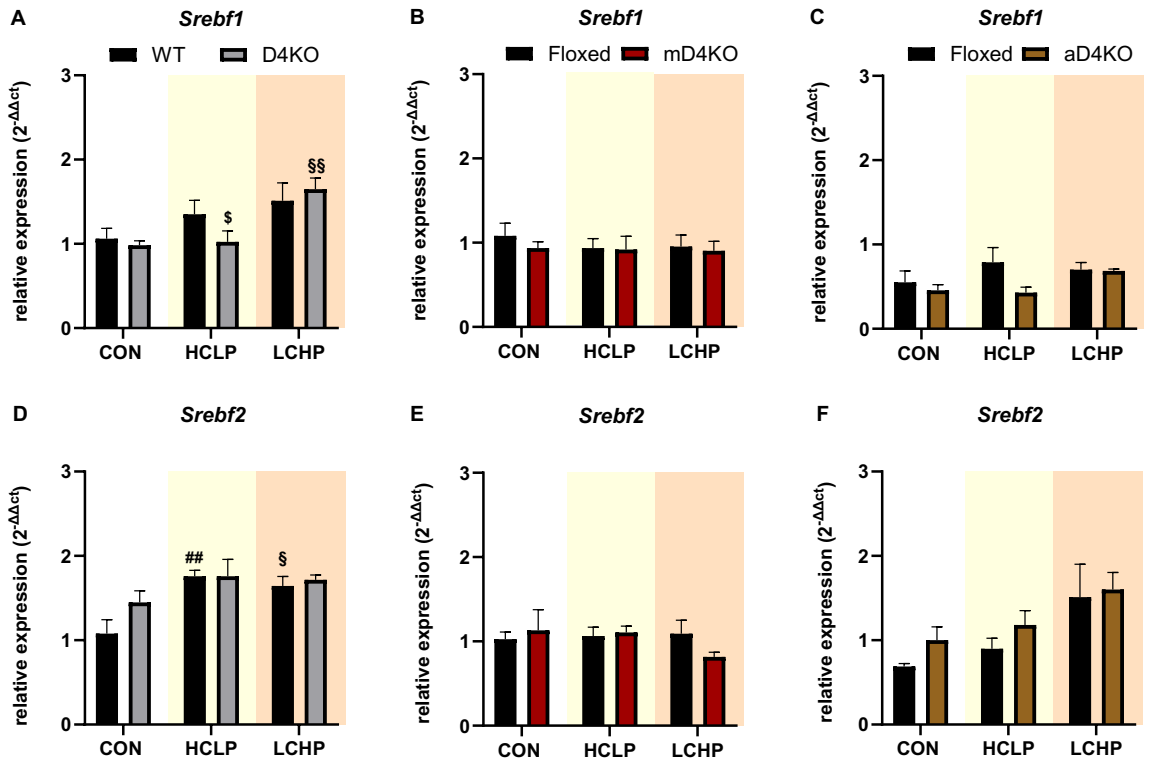


Figure 6: Gene expression levels of *Srebf1* and *Srebf2* in the liver of global and tissue-specific-D4KO mice.
Relative mRNA expression of Sterol regulatory element-binding protein 1 (*Srebf1*) and Sterol regulatory element-binding protein 2 (*Srebf2*) in D4KO (**A, D**), mD4KO (**B, E**), and aD4KO (**C, F**) mice and their WT/ floxed littermates subjected to a CON, HCLP or LCHP diet (n=6-9). Normalization was accomplished by applying the ΔΔCT-method, using H3f3a as the reference gene. Data shown represent mean ± SEM. Two-way ANOVA with Bonferroni-correction was used for statistical analysis. ##p <0.01, CON vs. HCLP. §p <0.05, §§p <0.01, CON vs. LCHP. $p <0.05, HCLP vs. LCHP.

Fatty acid synthase (FASN) is a key enzyme involved in the biosynthesis of saturated long-chain fatty acids from acetyl-CoA and malonyl-CoA [70].

In control animals, the abundance of FASN was significantly reduced on both the HCLP and LCLP diets compared to the CON diet, as shown in Fig. 7.A and C. Similar patterns were observed in D4KO, mD4KO, and aD4KO mice (Fig. 7.A–C). Additionally, FASN abundance was significantly lower in D4KO mice than in WT controls under HCLP feeding (Fig. 7.A). Figure 7.C shows that protein abundance in aD4KO mice was significantly lower on the CON diet compared to their floxed littermates.

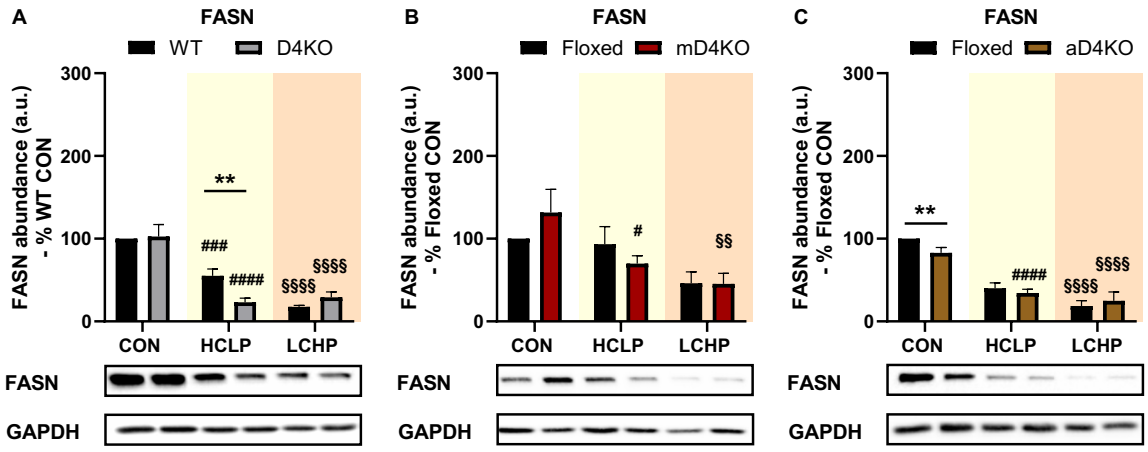


Figure 7: Protein abundance of FASN in the liver of global and tissue-specific D4KO mice. Fatty acid synthase (FASN) abundance in D4KO (**A**), mD4KO (**B**), and aD4KO (**C**) mice and their WT/ floxed littermates subjected to a CON, HCLP or LCHP diet (n=6-9). Protein abundance was normalized to GAPDH. Data shown represent mean ± SEM. Two-way ANOVA with Bonferroni-correction was used for statistical analysis. **p <0.01, KO vs. WT. #p <0.05, ###p <0.001, #### <0.0001, CON vs. HCLP. §§p <0.01, §§§§p <0.0001, CON vs. LCHP.

3.1.1.2 Impact of diets on expression levels of genes involved in modification of fatty acids (desaturation and elongation) in the liver of Tbc1d4-deficient mice

In this study, hepatic expression levels of genes involved in fatty acid modification were assessed by qPCR in *Tbc1d4*-deficient mice (2.2.1.3).

Stearoyl-CoA Desaturase 1 (*Scd1*) encodes a desaturase that generates monounsaturated fatty acids [71].

Hepatic *Scd1* expression levels were significantly reduced in control animals on both the HCLP and LCHP diets compared to the CON diet (Fig. 8.A–C). The same pattern was observed in D4KO, mD4KO, and aD4KO mice, with significantly lower expression levels on both HCLP and LCHP diets relative to CON (Fig. 8.A–C). Additionally, *Scd1* expression levels were significantly higher in D4KO mice compared to WT controls under CON feeding (Fig. 8.A). In contrast, aD4KO mice showed significantly lower *Scd1* expression levels compared to floxed controls on the CON diet (Fig. 8.C).

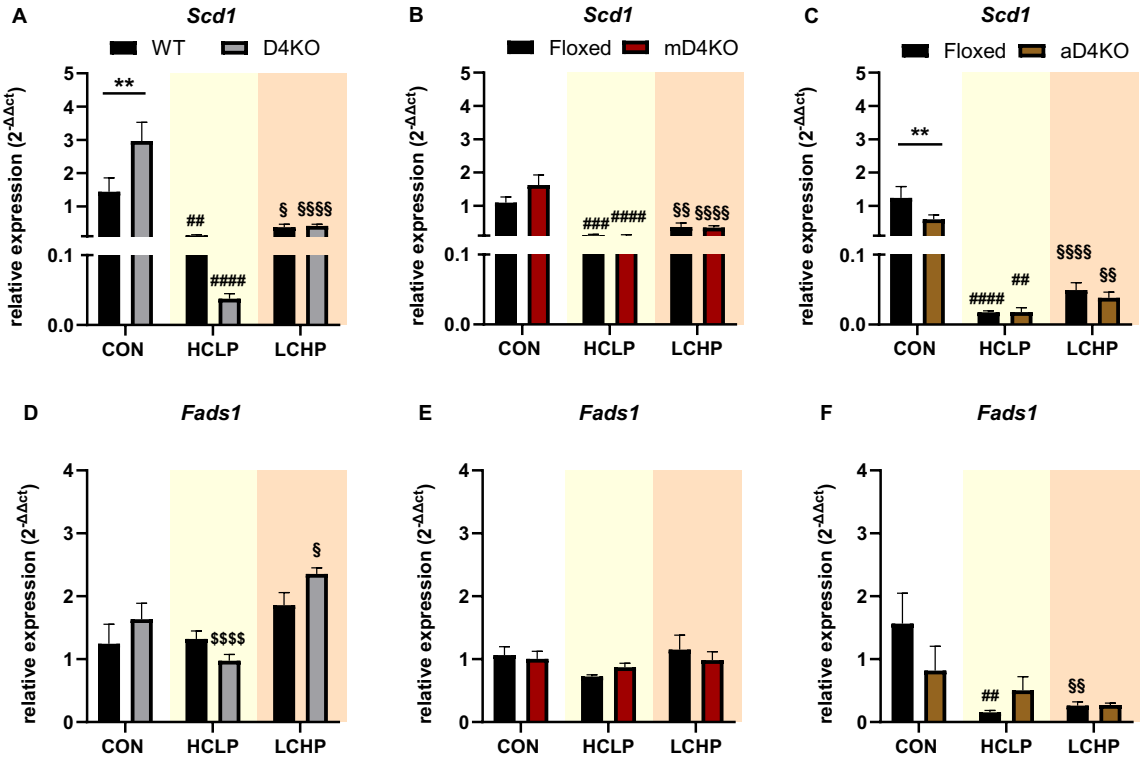
Fatty Acid Desaturase 1 (*Fads1*) encodes a desaturase enzyme that is involved in the production of polyunsaturated fatty acids [72].

In control animals, no significant changes in *Fads1* expression levels were observed across diets in WT and floxed mice (Fig. 8.D and E). However, Fig. 8.F shows that a significant reduction in *Fads1* expression occured in floxed mice on both the HCLP and LCHP diets compared to the CON diet. In D4KO mice, expression levels were

significantly increased on the LCHP diet and decreased on the HCLP diet when compared to the CON diet (Fig. 8.D). There were no statistically significant differences in *Fads1* expression levels between genotypes within the same dietary group.

Elongation of Very Long Chain Fatty Acids Protein 6 (*Elovl6*) encodes for an enzyme that is responsible for the elongation of saturated and monounsaturated fatty acids [73].

No significant changes in *Elovl6* expression levels were observed in WT and floxed mice across diets (Fig. 8.G and H). However, Fig. 8.I shows a reduction in *Elovl6* expression levels on both the HCLP and LCHP diets compared to the CON diet. *Elovl6* expression levels were significantly increased in both mD4KO and aD4KO mice on the HCLP diet compared to the LCHP diet (Fig. 8.H and I). There were no statistically significant differences in *Elovl6* expression levels between genotypes within the same dietary group.



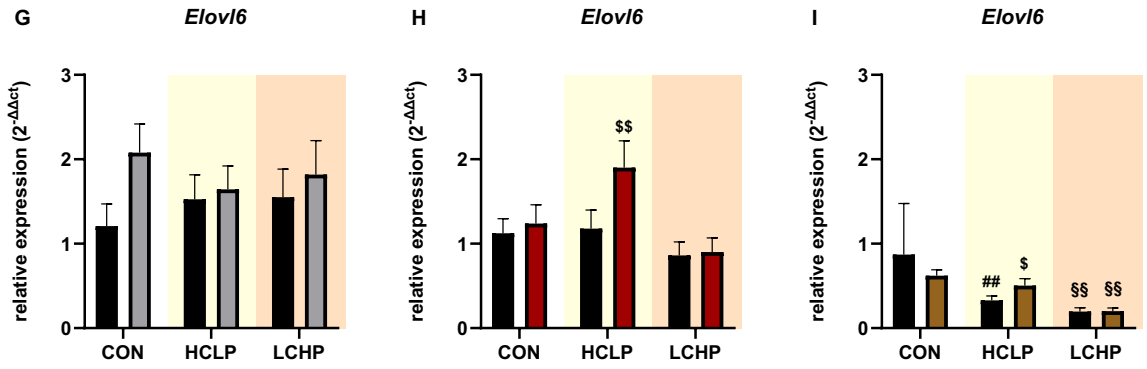


Figure 8: Gene expression levels of *Scd1*, *Fads1*, and *Elovl6* in the liver of global and tissue-specific-D4KO mice.
Relative mRNA expression of Steaoryl-CoA desaturase 1 (*Scd1*), Fatty acid desaturase (*Fads1*) and Elongation of very long chain fatty acids 6 (*Elovl6*) in D4KO (**A, D, G**), mD4KO (**B, E, H**), and aD4KO (**C, F, I**) mice and their WT/ floxed littermates subjected to a CON, HCLP or LCHP diet (n=6-9). Normalization was accomplished by applying the ΔΔCT-method, using H3f3a as the reference gene. Data shown represent mean ± SEM. Two-way ANOVA with Bonferroni- correction was used for statistical analysis. **p <0.01 KO vs. WT. ##p <0.01, ###p <0.001, #### <0.0001, CON vs. HCLP. §p <0.05, §§p <0.01, §§§§p <0.0001, CON vs. LCHP. $p <0.05, $$$$p <0.0001, HCLP vs. LCHP.

3.1.1.3 Impact of diets on expression levels of genes involved in fatty acid oxidation in the liver of Tbc1d4-deficient mice

Tbc1d4-deficient mice have been shown to exhibit a metabolic shift from utilizing glucose to oxidizing fatty acids [51]. This study quantified the hepatic expression levels of genes involved in fatty acid oxidation using qPCR (2.2.1.3).

Acyl-CoA thioesterase 2 (*Acot2*) functions as a catalyst for the hydrolysis of acyl-CoA thioesters, resulting in the liberation of free fatty acids and CoA. This process plays a pivotal role in regulating beta oxidation [74].

A significant increase in *Acot2* expression levels were observed in control animals on the HCLP diet compared to the LCHP and CON diets (see Fig. 9.A and B). A similar trend was observed in floxed controls in Fig. 9.C. D4KO, mD4KO, and aD4KO mice showed a comparable pattern, with significantly higher *Acot2* expression levels on the HCLP diet compared to the LCHP diet (Fig. 9.A–C). There were no statistically significant differences in *Acot2* expression levels between genotypes within the same dietary group.

Carnitine palmitoyltransferase 1 (*Cpt1*) plays a pivotal role in regulating the rate-limiting step of β-oxidation by facilitating the transport of long-chain fatty acids into the mitochondria. This is achieved by converting the acyl-CoA of the fatty acids to acyl-carnitine, which is then able to cross the mitochondrial membrane [74].

Regardless of dietary interventions, no changes in gene expression levels were observed in either control animals or KO mice (Fig. 9.D-F). D4KO mice showed significantly increased *Cpt1* expression levels on the HCLP diet compared to WT animals on the same diet (Fig. 9.D).

Carnitine palmitoyltransferase 2 (*Cpt2*) catalyzes the conversion of acyl-carnitine back into acyl-CoA within the mitochondrial matrix, thereby facilitating the entry of fatty acids into β-oxidation [75].

No notable differences in *Cpt2* expression levels were observed between the dietary groups or between genotypes (Fig. 9.G-I).

Peroxisome Proliferator-Activated Receptor Alpha (*Ppara*) is a nuclear receptor that regulates the expression of genes involved in lipid metabolism, including beta oxidation [76].

In control animals, *Ppara* expression levels were significantly elevated in WT mice on the LCHP diet compared to both the HCLP and CON diets (Fig. 9.J). In contrast, floxed mice showed significantly reduced *Ppara* expression levels on both HCLP and LCHP diets compared to the CON diet (Fig. 9.L). In D4KO mice, a similar pattern to that of WT controls was observed, with increased expression levels on the LCHP diet relative to the other diets (Fig. 9.J). Additionally, *Ppara* expression levels were significantly reduced in aD4KO mice compared to floxed controls under CON feeding (Fig. 9.L).

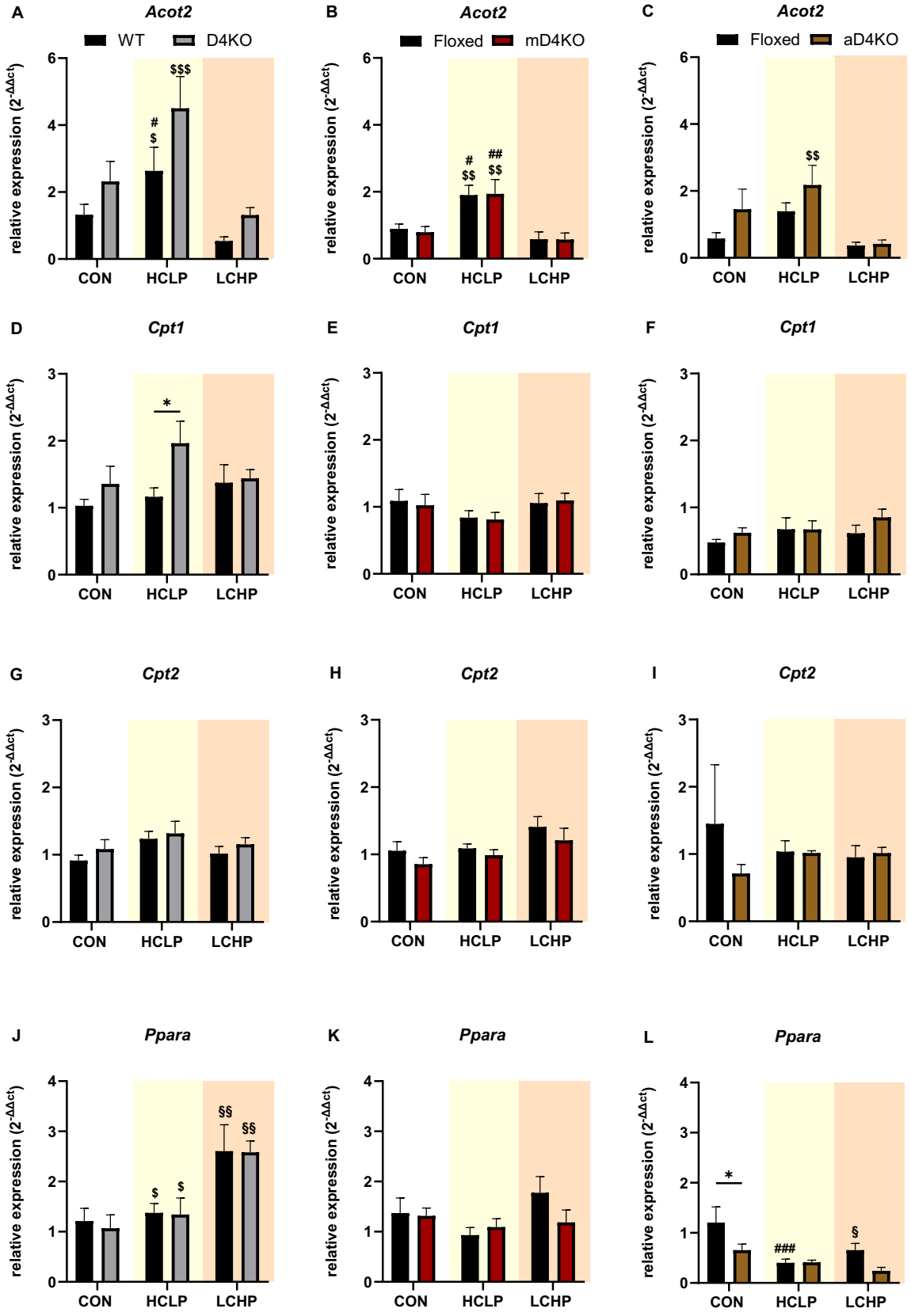


Figure 9: Gene expression levels of *Acot2*, *Cpt1*, *Cpt2*, and *Ppara* in the liver of global and tissue-specific-D4KO mice.
Relative mRNA expression of Acyl-CoA Thioesterase 2 (*Acot2*), Carinitine palmitoyltransferase 1 (*Cpt1*), Carinitine palmitoyltransferase 2 (*Cpt2*) and Peroxisome proliferator-activated receptor alpha (*Ppara*) in D4KO (**A, D, G, J**), mD4KO (**B, E, H, K**), and aD4KO (**C, F, I, L**) mice and their WT/ floxed littermates

subjected to a CON, HCLP or LCHP diet (n=6-9). Normalization was accomplished by applying the ΔΔCT-method, using H3f3a as the reference gene. Data shown represent mean ± SEM. Two-way ANOVA with Bonferroni- correction was used for statistical analysis. *p <0,05, KO vs. WT. #p <0,05, ##p <0.01, ###p < 0.001, CON vs. HCLP. §p <0.05, §§p <0.01, CON vs. LCHP. $p <0.05, $$p <0.01, $$$p <0.001, HCLP vs. LCHP.

3.2 Hepatic triglyceride levels of Tbc1d4-deficient mice fed diets of differing macronutrient ratios

MASLD is a prevalent diagnosis among patients with T2D [77]. The quantity of TGs in the liver can serve as an indicator of the presence of hepatic steatosis, which can progress to MASLD [78]. The present study examined TG levels in the livers of *Tbc1d4*-deficient mice fed a CON, HCLP, and LCHP diet. To quantify TG levels in the liver, total and free glycerol levels were measured (2.2.2.5).

In control animals, free glycerol levels were significantly reduced in WT mice on the LCHP diet compared to the CON diet (Fig. 10.A). No significant dietary differences were observed in total glycerol or TG levels in WT mice (Fig. 10.B and C).

In D4KO mice, total glycerol and TG levels were significantly increased on the HCLP diet compared to both the LCHP and CON diets (Fig. 10.B and C). No significant changes in free glycerol levels were observed in D4KO mice across diets (Fig. 10.A).

Additionally, total glycerol and TG levels showed a tendency to be higher in D4KO mice compared to WT controls under HCLP feeding (Fig. 10.B and C).

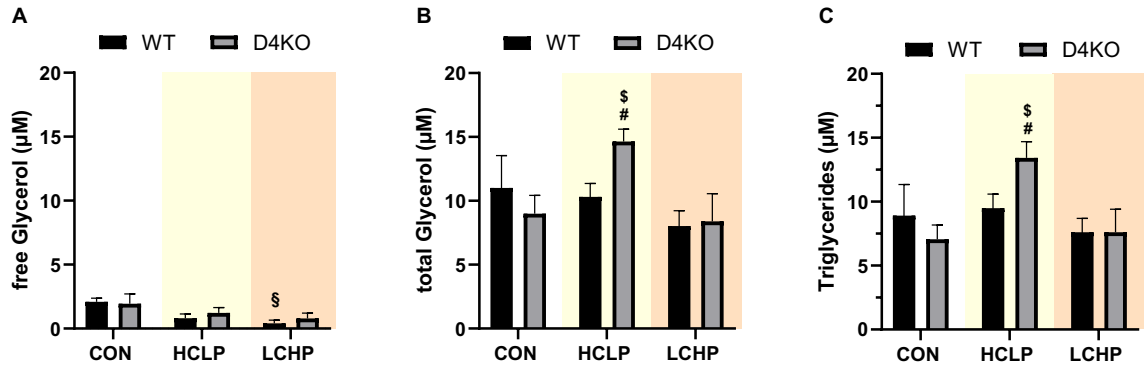


Figure 10: Glycerol and triglyceride levels in the liver of global D4KO.
Free Glycerol (A), total Glycerol (B) and Triglyceride (C) levels (in µM) of D4KO mice and their WT littermates subjected to a CON, HCLP, and LCHP diet. Data represent mean ± SEM. N = 2-6. Statistical analysis with two-way ANOVA with Bonferroni-correction. **p <0.01, WT vs. D4KO, #p <0.05, ##p <0.01, CON vs. HCLP, §p <0.05, §§p <0.01, CON vs. LCHP, $p <0.05, HCLP vs. LCHP.

3.3 Impact of differing dietary macronutrient ratios on key regulators of glucose metabolism in the liver of Tbc1d4-deficient mice

To determine the impact that different dietary macronutrient ratios have on glucose metabolism of *Tbc1d4*-deficient mice, studies were conducted at both gene and protein levels.

3.3.1 Impact of differing dietary macronutrient ratios on expression levels of genes and abundance of proteins regulating hepatic gluconeogenesis in the liver of Tbc1d4-deficient mice

Tbc1d4-deficiency has been associated with postprandial hyperglycemia in both humans and mice [56, 61]. In this study, hepatic expression levels of key gluconeogenic genes were measured in *Tbc1d4*-deficient mice using qPCR (2.2.1.3) and Western Blot (2.2.2.4).

Phosphoenolpyruvate carboxykinase 1 (PCK1) is a cytoplasmic enzyme that plays a pivotal role in gluconeogenesis by catalyzing the conversion of oxaloacetate to phosphoenolpyruvate [79].

No significant alterations in *Pck1* expression levels were observed in control animals across dietary conditions (Fig. 11.A–C). In D4KO mice, *Pck1* expression levels were significantly elevated on the HCLP diet compared to the LCHP diet, but not compared to the CON diet (Fig. 11.A). Additionally, expression levels were significantly higher in D4KO mice than in WT controls under HCLP feeding (Fig. 11.A). A similar tendency toward increased expression levels on the HCLP diet were observed in mD4KO and aD4KO mice compared to their respective controls (Fig. 11.B and C).

FoxO1 is a transcription factor that plays a crucial role in regulating various physiological processes, including glucose metabolism [80].

In control animals, *FoxO1* expression levels were significantly increased in WT mice on the HCLP diet compared to the CON diet, with a tendency toward increased expression levels compared to the LCHP diet (Fig. 11.D). Furthermore, there was a tendency towards increased *FoxO1* expression levels on the LCHP diet, which was significant in the floxed mice when compared to those on the HCLP diet (Fig. 11.F). No significant dietary differences were observed in D4KO, mD4KO, or aD4KO mice

(Fig. 11.D–F). However, *FoxO1* expression levels showed a tendency to be lower in D4KO mice compared to WT controls under HCLP feeding (Fig. 11.D).

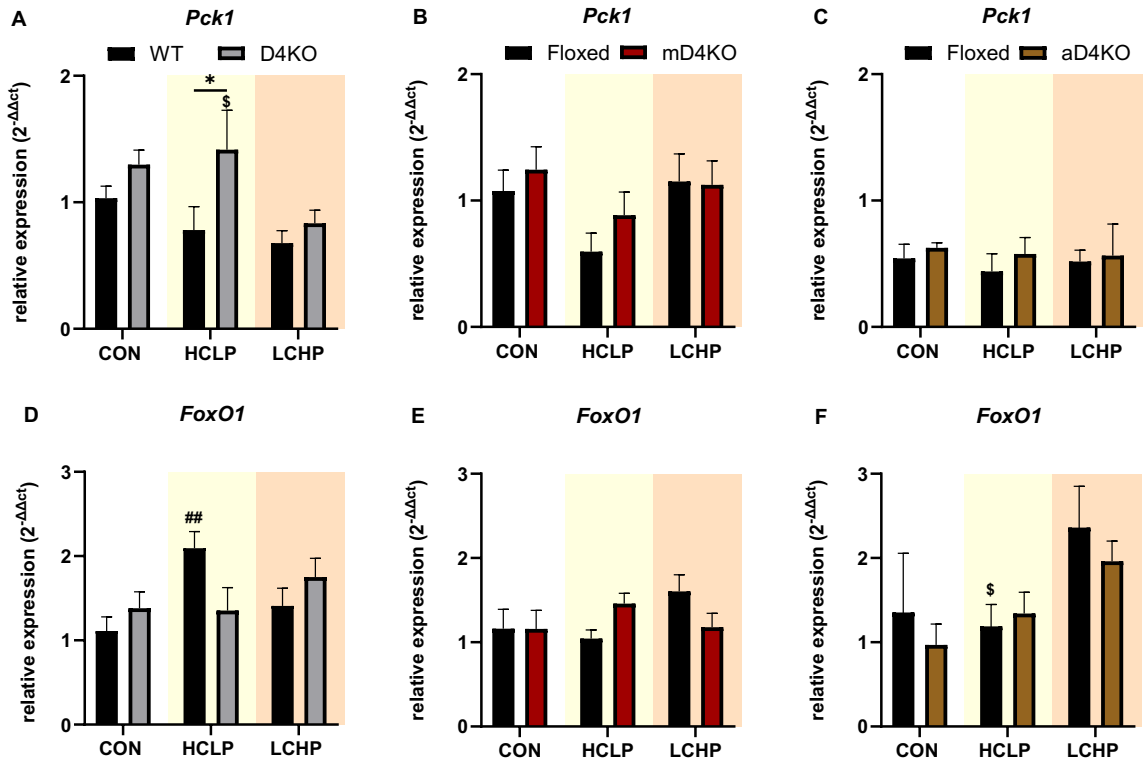


Figure 11: Gene expression levels of *Pck1* and *FoxO1* in the liver of global and tissue-specific-D4KO mice.
Relative mRNA expression of Phoshoenolpyruvate carboxykinsae 1 (*Pck1*) and Forkhead box O1 (*FoxO1*) in D4KO (**A, D**), mD4KO (**B, E**), and aD4KO (**C, F**) mice and their WT/ floxed littermates subjected to a CON, HCLP or LCHP diet (n=6-9). Normalization was accomplished by applying the ΔΔCT-method, using H3f3a as the reference gene. Data shown represent mean ± SEM. Two-way ANOVA with Bonferroni- correction was used for statistical analysis. * p < 0.05, KO vs. WT. ##p <0.01, CON vs. HCLP. $p <0.05 HCLP vs. LCHP.

PCK1 abundance was significantly decreased on the HCLP diet relative to the LCHP diet in both WT and floxed mice (Fig. 12.A and B). No significant changes in PCK1 levels were observed across dietary conditions in D4KO, mD4KO, or aD4KO mice (Fig. 12.A–C). However, a tendency toward increased protein abundance in D4KO and aD4KO mice compared to their respective control groups was observed (Fig. 12.A and C).

Phosphoenolpyruvate Carboxykinase 2 (PCK2) catalyzes the conversion of oxaloacetate to phosphoenolpyruvate in the mitochondria, thereby regulating gluconeogenesis [81].

In control animals, PCK2 abundance was significantly increased in floxed mice on the HCLP diet compared to both the CON and LCHP diets (Fig. 12.F). A similar tendency

toward increased abundance on the HCLP diet was observed in WT and floxed mice in Fig. 12.A and B.

In D4KO mice, PCK2 abundance was significantly higher on the HCLP diet compared to the LCHP diet (Fig. 12.A). A similar pattern was observed in mD4KO and aD4KO mice (Fig. 12.B and C). There were no statistically significant differences in PCK2 abundance between genotypes within the same dietary group.

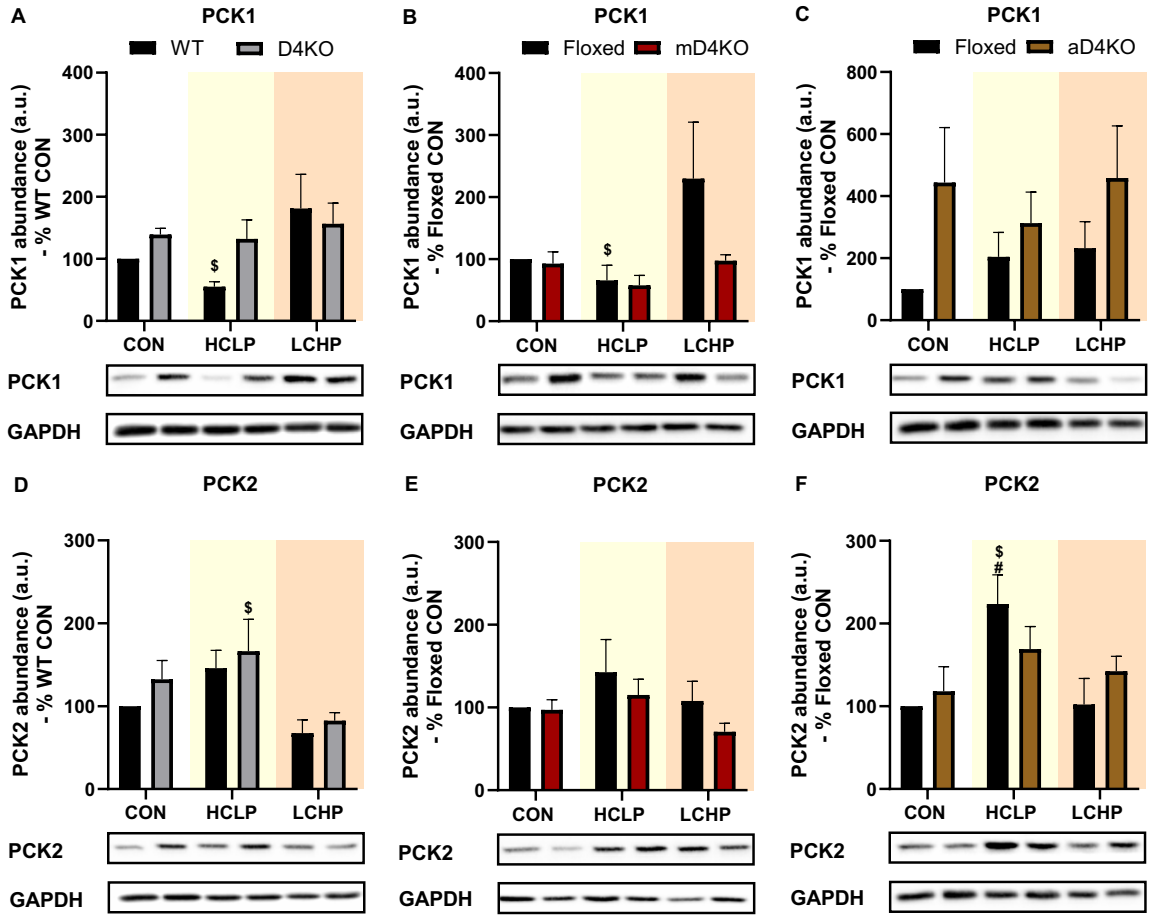


Figure 12: Protein abundance of PCK1 and PCK2 in the liver of global and tissue-specific-D4KO mice.
Phoshoenolpyruvate carboxykinsae 1 (PCK1) and Phoshoenolpyruvate carboxykinsae 2 (PCK2) abundance in D4KO (**A, D**), mD4KO (**B, E**), and aD4KO (**C, F**) mice and their WT/ floxed littermates subjected to a CON, HCLP or LCHP diet (n=6-9). Protein abundance was normalized to GAPDH. Data shown represent mean ± SEM. Two-way ANOVA with Bonferroni-correction was used for statistical analysis. #p <0.05, CON vs. HCLP. $p <0.05, HCLP vs. LCHP.

3.3.2 Impact of differing dietary macronutrient ratios on expression levels of genes and protein abundance of regulators of glycolysis and lipogenesis in the liver of Tbc1d4-deficient mice

In this study, hepatic gene expression levels of key glycolytic and lipogenic regulators were quantified by qPCR (2.2.1.3), and corresponding protein levels were assessed by Western blotting (2.2.2.4) in *Tbc1d4*-deficient mice.

MLX interacting protein-like (*Mlxipl*) is a transcription factor that regulates the expression of genes involved in glycolysis and lipogenesis, thereby promoting the conversion of glucose into pyruvate and the synthesis of fatty acids. The *Mlxipl* gene encodes ChREBP1 [82].

In control animals, *Mlxipl* expression levels were significantly increased on the HCLP diet compared to both the LCHP and CON diets in WT and floxed mice (Fig. 13.A and B). In D4KO and mD4KO mice, a similar trend was observed, with expression levels significantly elevated on the HCLP diet compared to the CON diet (Fig. 13.A and B). Across all genotypes, a reduction in *Mlxipl* expression levels were observed on the LCHP diet relative to other dietary conditions. There were no statistically significant differences in *Mlxipl* expression levels between genotypes within the same dietary group.

Malic enzyme 1 (*Me1*) encodes for an enzyme that generates nicotinamide adenine dinucleotide phosphate (NADPH) by reducing malate to pyruvate. This is a crucial step in fatty acid synthesis and serves to integrate glycolysis with fatty acid synthesis [83].

In control animals, *Me1* expression levels were increased on the HCLP diet compared to the LCHP diet in both WT and floxed mice (Fig. 13.D and E). In floxed mice, expression levels were also significantly higher on the HCLP diet compared to the CON diet (Fig. 13.E). Across all genotypes, a reduction in *Me1* expression levels were observed on the LCHP diet relative to other dietary conditions, with significant differences in D4KO and mD4KO mice when compared to the HCLP diet (Fig. 13.D and E). Furthermore, *Me1* expression levels in mD4KO mice were considerably higher than those in floxed controls under CON feeding (Fig. 13.E). Conversely, aD4KO mice exhibited significantly reduced expression levels compared to floxed controls on the CON diet (Fig. 13.F).

Pyruvate Kinase Liver/Red Blood Cell (*Pklr*) encodes for the enzyme that catalyzes the final step in glycolysis, generating pyruvate and adenosine triphosphate (ATP) [84].

Pklr expression levels were significantly increased in both control animals and knock out mice on the HCLP diet compared to other dietary groups (Fig. 13.G-I). A significant

increase could be observed in mD4KO and aD4KO mice on the HCLP diet compared to the LCHP diet (Fig. 13.H-I). There were no statistically significant differences in *Pklr* expression levels between genotypes within the same dietary group.

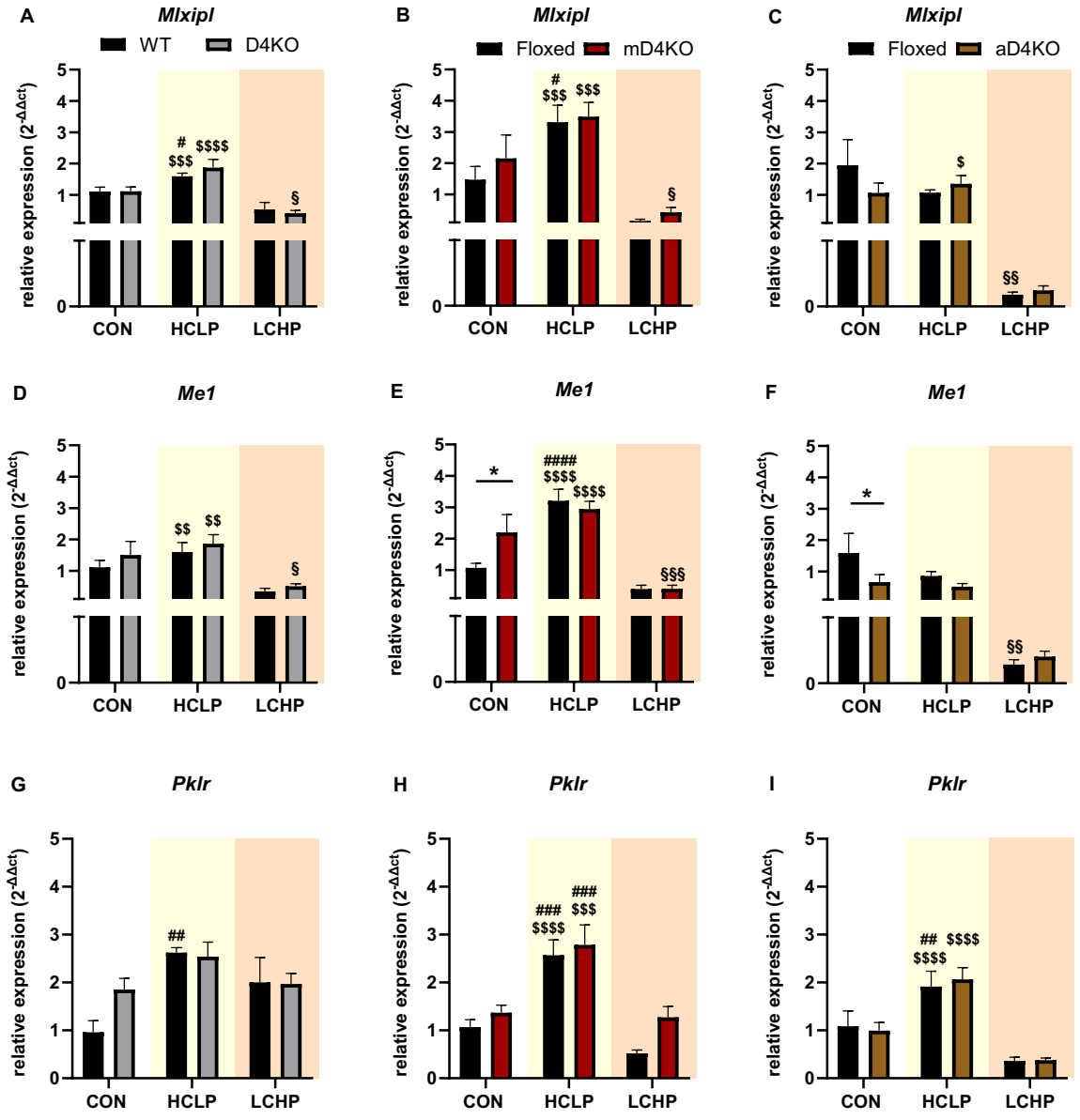


Figure 13: Gene expression levels of *Mlxipl*, *Me1*, and *Pklr* in the liver of global and tissue-specific-D4KO mice.
Relative mRNA expression of MLX Interacting Protein Like protein (*Mlxipl*), Malic Enzyme 1 (*Me1*) and Pyruvate kinase L/R (*Pklr*) in D4KO (**A, D, G**), mD4KO (**B, E, H**), and aD4KO (**C, F, I**) mice and their WT/ floxed littermates subjected to a CON, HCLP or LCHP diet (n=6-9). Normalization was accomplished by applying the ΔΔCT-method, using H3f3a as the reference gene. Data shown represent mean ± SEM. Two-way ANOVA with Bonferroni- correction was used for statistical analysis. *p <0.05, KO vs. WT. #p <0.05, ##p <0.01, ###p <0.001, ####p <0.0001, CON vs. HCLP. §p <0.05, §§p <0.01, §§§ <0.001, CON vs. LCHP. $$p <0.01, $$$p <0.001, $$$$p <0.0001, HCLP vs. LCHP.

3.3.3 *Impact of differing dietary macronutrient ratios on mRNA expression levels of key factors regulating glycogen synthesis in the liver of Tbc1d4-deficient mice*

Glycogen synthase 2 (GYS2) catalyzes the conversion of glucose to glycogen, which can then be stored in the liver [85].

GYS2 abundance in WT and floxed mice remained unchanged across dietary conditions (Fig. 14.A–C). In D4KO and mD4KO mice, no significant differences in protein abundance were observed in response to dietary intervention (Fig. 14.A and B). In aD4KO mice, GYS2 abundance was significantly increased on the HCLP diet compared to the LCHP diet (Fig. 14.C). Additionally, a tendency toward increased protein abundance on the HCLP diet was observed in both D4KO and aD4KO mice when compared to WT and floxed controls, respectively (Fig. 14.A and C).

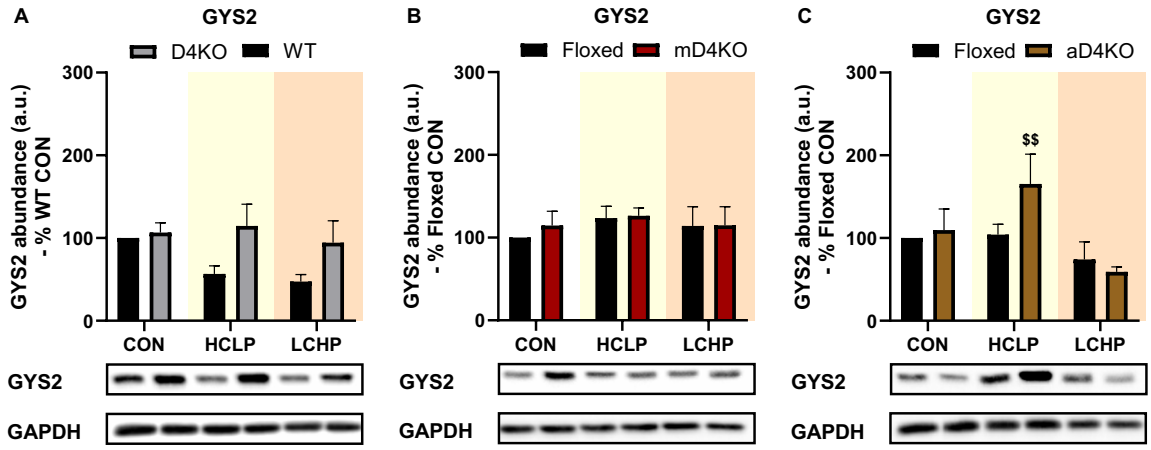


Figure 14: Protein abundance of GYS2 in the liver of global and tissue-specific-D4KO mice. Glycogen synthase 2 (GYS2) abundance in D4KO (**A**), mD4KO (**B**), and aD4KO (**C**) mice and their WT/ floxed littermates subjected to a CON, HCLP or LCHP diet (n=6-9). Protein abundance was normalized to GAPDH. Data shown represent mean ± SEM. Two-way ANOVA with Bonferroni-correction was used for statistical analysis. $$p <0.01, HCLP vs. LCHP.

3.3.4 *Impact of differing dietary macronutrient ratios on expression levels of genes involved in the regulation of insulin signaling in the liver of Tbc1d4-deficient mice*

In *Tbc1d4*-deficiency, insulin-stimulated GLUT4 vesicle trafficking is impaired [44]. This study quantified the hepatic gene expression levels of key insulin signaling regulators by qPCR (2.2.1.3).

Sirtuin1 (*Sirt1*) encodes for a NAD+-dependent deacetylase that has been demonstrated to promote gluconeogenesis in the liver and to stimulate insulin signaling [86].

In control animals, *Sirt1* expression levels remained unchanged across dietary conditions in WT and floxed mice (Fig. 15.A and C). However, in Fig. 15.B, floxed mice showed a significant increase in gene expression levels on the LCHP diet compared to both the HCLP and CON diets. In D4KO, mD4KO, and aD4KO mice, no alterations in *Sirt1* expression levels were observed across dietary interventions (Fig. 15.A–C). There were no statistically significant differences in *Sirt1* expression levels between genotypes within the same dietary group.

TBC1 Domain Family Member 1 (*Tbc1d1*) encodes a protein that plays a regulatory role in glucose and lipid metabolism [51].

In Fig. 15.D, *Tbc1d1* expression levels were significantly increased in WT mice on the HCLP diet compared to the CON diet. In In Fig. 15.F, expression levels were significantly reduced in floxed mice on the LCHP diet compared to the CON diet. In D4KO, mD4KO, and aD4KO mice, *Tbc1d1* expression levels remained unchanged across dietary interventions (Fig. 15.D–F). Additionally, *Tbc1d1* expression levels were significantly reduced in aD4KO mice compared to floxed controls under CON feeding (Fig. 15.F).

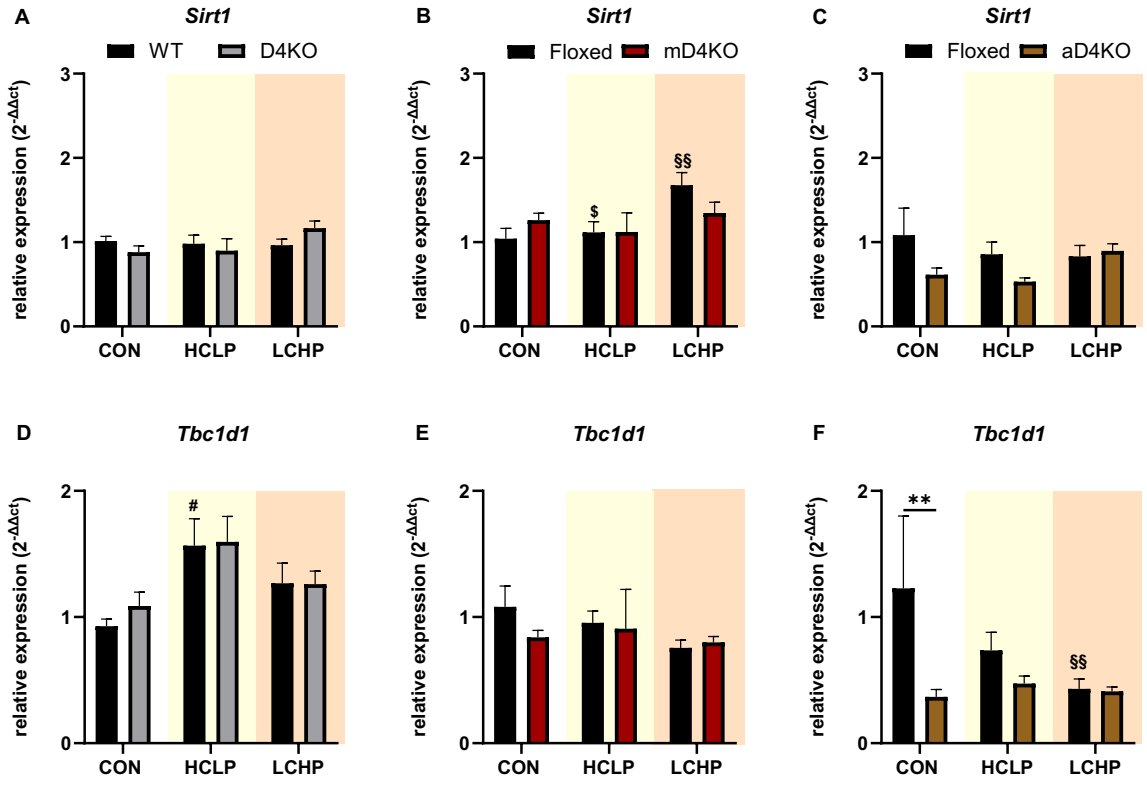


Figure 15: Gene expression levels of *Sirt1* and *Tbc1d1* in the liver of global and tissue-specific-D4KO mice.

Relative mRNA expression of Sirtuin 1 (*Sirt1*) and TBC1 Domain Family Member 1 (*Tbc1d1*) in D4KO (**A, C**), mD4KO (**B, E**), and aD4KO (**C, F**) mice and their WT/ floxed littermates subjected to a CON, HCLP or LCHP diet (n=6-9). Normalization was accomplished by applying the ΔΔCT-method, using H3f3a as the reference gene. Data shown represent mean ± SEM. Two-way ANOVA with Bonferroni-correction was used for statistical analysis. **p <0.01, KO vs. WT. #p <0.05, CON vs. HCLP. §§p <0.01, CON vs. LCHP. $p <0.05, HCLP vs. LCHP.

4 Discussion

TBC1D4 is a RabGAP that promotes insulin-stimulated GLUT4 translocation and glucose uptake into skeletal muscle and adipose tissue [50]. This process regulates systemic glucose and lipid metabolism [52]. A nonsense mutation (*p.Arg684Ter*) in *TBC1D4* that is specific to skeletal muscle and common in Arctic populations is associated with postprandial hyperglycemia, insulin resistance, and a specific subtype of T2D [58]. This mutation may reflect an adaptation to a traditional high-fat, high-protein, low-carbohydrate diet. The rising prevalence of T2D in this population may be linked to lifestyle changes toward a Western diet [60]. Mouse models with *Tbc1d4* knockout exhibit a similar phenotype, including postprandial hyperglycemia and reduced GLUT4 abundance in insulin-sensitive tissues [56].

Previous results from our group demonstrated that D4KO and aD4KO mice show postprandial hyperglycemia and hyperinsulinemia when subjected to a Western, HCLP diet. Feeding the mice a LCHP diet prevented postprandial hyperglycemia and improved skeletal muscle insulin sensitivity. Interestingly, Dr. Scheel observed elevated levels of fasting plasma ketone bodies in global D4KO and aD4KO mice, but not mD4KO mice, subjected to a HCLP diet, which were normalized by subjecting the mice to an LCHP diet [62]. The elevation of plasma ketone bodies indicates an involvement of the liver and a shift from glucose to lipid metabolism in response to D4-deficiency. Furthermore, the observation that only global D4KO and aD4KO mice exhibited elevated plasma ketone bodies, but not mD4KO mice, suggests an interplay between insulin-responsive tissues and the liver.

These findings prompted further investigation into the role of hepatic energy substrate metabolism of D4KO mice and the impact of peripheral insulin-responsive tissues on glucose and lipid metabolism of these mice. The focus was on the impact of different macronutrient ratios, with special regard to the potentially protective effects of a LCHP diet. Additionally, the role of different diets on lipid accumulation in *Tbc1d4*-deficient mice was further investigated.

4.1 A LCHP diet exerts protective effects on hepatic lipid accumulation in Tbc1d4-deficiency

Downregulation of key hepatic lipogenic genes in *Tbc1d4*-deficient mice fed a LCHP diet suggests that this dietary intervention has protective effects against hepatic lipid accumulation. These gene expression patterns, together with a reduced hepatic triglyceride content, highlight the significance of macronutrient composition in regulating liver metabolism when peripheral insulin signaling is impaired.

A diet comprising a high proportion of carbohydrates has been demonstrated to induce DNL primarily via activation of the glucose-responsive enzyme ChREBP. Enhanced DNL contributes to hepatic lipid deposition and the pathogenesis of MASLD [22].

In the present study, D4KO mice exhibited a significant increase in hepatic TG accumulation under HCLP feeding compared to both LCHP and control diets, indicating that carbohydrate restriction ameliorates hepatic steatosis and therefore its complications, including MASLD, in these mice.

At the molecular level, this dietary effect was accompanied by changes in the expression of enzymes involved in lipid metabolism. ACC1 plays a pivotal role in fatty acid synthesis, acting as a crucial enzyme in lipid metabolism. A previous study has demonstrated that *Acc1* is upregulated in patients with MASLD, and that the inhibition of the gene is associated with improvements in hepatic steatosis and fibrosis [87]. The present study demonstrates that hepatic *Acc1* expression levels are increased in mD4KO and aD4KO mice that have been fed a HCLP diet, in comparison to those that have been fed a LCHP diet. The reduced expression levels observed on the LCHP diet indicate that this dietary regimen may confer advantageous effects on hepatic lipid content, which could potentially attenuate the development of MASLD in *Tbc1d4* knockdown models. This finding emphasizes the idea of a complex interplay between peripheral tissues and the liver in energy substrate metabolism.

ME1 catalyzes the conversion of malate to pyruvate, generating NADPH for fatty acid synthesis, and therefore links glycolysis to lipogenesis [83]. In a previous study, a global *Me1* knockout was observed to protect male C57BL/6 mice from high-fat diet-induced obesity and its associated complications, including hyperinsulinemia and hepatic steatosis [88]. The present study demonstrated significantly elevated *Me1* expression levels in global D4KO and mD4KO mice fed a HCLP diet in comparison to

a LCHP diet. A reduction in gene expression levels on a LCHP diet suggest that this diet may exert a protective effect on hepatic lipid metabolism and may also prevent hepatic lipid accumulation in *Tbc1d4*-deficient mice. Furthermore, the dissimilarities in gene expression between the tissues provide additional evidence for an interplay of these tissues in metabolic processes.

Para is a transcription factor that plays a significant role in lipid metabolism by regulating the expression of genes involved in fatty acid oxidation [89]. A previous study demonstrated that the deletion of hepatic *Ppara* resulted in impaired lipid metabolism and hepatic lipid accumulation during fasting in mice [90]. The current study demonstrates a notable decline in hepatic *Ppara* expression levels in global D4KO mice fed a HCLP diet when compared to a LCHP diet. These findings further indicate possible protective effects of a LCHP diet, compared to a HCLP diet, on lipid metabolism and the development of MASLD.

FADS1 is responsible for the generation of ω-3 and ω-6 PUFAs [72]. Prior research has indicated a correlation between reduced *Fads1* expression levels and hepatic lipid accumulation [91]. The present study demonstrated that *Fads1* expression levels were diminished in global D4KO mice fed a HCLP diet when compared to a LCHP diet, suggesting that a HCLP diet exerts deleterious effects on hepatic lipid accumulation in global *Tbc1d4*-deficient mice. Conversely, the results indicate that a LCHP exerts beneficial effects on lipid metabolism and hepatic fat accumulation in global *Tbc1d4*-deficiency.

The findings collectively demonstrate that *Tbc1d4* deficiency leads to insulin resistance, which subsequently alters hepatic lipid metabolism through interorgan communication. A HCLP diet appears to result in an upregulation of lipogenic genes, which may consequently lead to hepatic lipid accumulation. A LCHP diet appears to counteract peripheral insulin resistance by downregulating lipogenic pathways and increasing fatty acid oxidation. This further highlights its potentially protective effects in the context of insulin-resistance and MASLD.

These results emphasize the complex interplay between insulin-responsive peripheral tissues and hepatic energy substrate metabolism in *Tbc1d4*-deficient states.

4.2 A HCLP causes a shift from glucose to lipid metabolism in Tbc1d4-deficiency

An increase in hepatic expression levels of genes associated with lipid catabolism in *Tbc1d4*-deficient mice fed a HCLP diet indicates a compensatory shift from glucose to lipid metabolism under conditions of peripheral insulin resistance. This response appears to be attenuated by a LCHP diet, suggesting an important role of macronutrient composition in regulating systemic metabolic adaptation in the context of *Tbc1d4*-deficiency.

ACOT2 is involved in fatty acid oxidation by catalyzing the hydrolysis of long-chain fatty acyl-CoA into free fatty acids and CoASH. Prior research has demonstrated a correlation between elevated *Acot2* activity and increased beta-oxidation of fatty acids [74]. The present study shows increased hepatic *Acot2* expression levels in D4KO, mD4KO, and aD4KO mice fed a HCLP diet compared to those provided a LCHP diet. The findings indicate that *Tbc1d4*-deficiency leads to increased lipid oxidation, particularly when carbohydrate availability is high. This is supported by the observation that the upregulation is consistent across all knockout models. Conversely, a reduction of *Acot2* expression levels under LCHP feeding suggests that under a low-carbohydrate diet, *Tbc1d4*-deficient mice are not reliant on lipid oxidation, indicating improved glucose utilization and peripheral insulin sensitivity.

The upregulation of *Acot2* in *Tbc1d4*-deficient mice may reflect a hepatic response to reduced glucose uptake in insulin-sensitive tissues. Despite glucose availability, insulin resistance limits glucose utilization in peripheral tissues, causing the liver to shift toward lipid oxidation as an alternative energy source.

Taken together, these findings indicate that *Tbc1d4*-deficiency promotes a shift from glucose to lipid metabolism, driven by peripheral insulin resistance. The upregulation of *Acot2* under HCLP conditions emphasizes the metabolic inflexibility of *Tbc1d4*-deficient mice. A downregulation on a LCHP diet highlights how dietary composition, specifically carbohydrate restriction, can partially restore glucose utilization and thereby metabolic flexibility.

4.3 Downregulation of Pklr on a LCHP diet potentially improves glucose metabolism and hepatic lipid accumulation in peripheral tissues of Tbc1d4-deficient mice

Reduced expression levels of *Pklr* in *Tbc1d4*-deficient mice fed a LCHP diet suggest a protective role of this dietary regimen in attenuating hepatic metabolic dysfunction. These findings align with previous studies demonstrating that suppression of *Pklr* improves glucose tolerance and reduces hepatic lipid accumulation, whereas its upregulation is associated with the progression of MASLD [92].

Pklr catalyzes the final step of glycolysis, converting phosphoenolpyruvate to pyruvate, generating substrates essential for both gluconeogenesis and DNL [84]. In the present study, hepatic *Pklr* expression levels were elevated in mD4KO and aD4KO mice on a HCLP diet but reduced under LCHP feeding. This indicates that a LCHP diet may attenuate DNL and hepatic lipid accumulation. Elevated *Pklr* expression levels under HCLP feeding likely reflect impaired peripheral glucose uptake, leading to increased hepatic glucose metabolism and lipogenesis. A LCHP diet may prevent this by enhancing insulin sensitivity and facilitating glucose uptake.

These findings suggest that *Tbc1d4*-deficiency alters hepatic glycolytic gene expression in response to diet. The absence of this effect in global knockouts underscores the role of inter-organ communication in regulating hepatic metabolism. The data support the hypothesis that carbohydrate restriction may help reduce the risk of MASLD and T2D in metabolically compromised conditions.

4.4 Reduced hepatic Elovl6 expression on a LCHP diet may indicate improved insulin sensitivity in peripheral tissues of Tbc1d4-deficient mice

Reduced *Elovl6* expression levels in *Tbc1d4*-deficient mice fed a LCHP diet suggest beneficial effects of this dietary intervention on glucose metabolism in insulin-sensitive tissues. *Elovl6* is involved in the elongation of saturated and monounsaturated fatty acids [73]. Previous studies have shown that suppression of *Elovl6* improves insulin sensitivity and glucose tolerance in models of T2D [93] [73].

In the present study, *Elovl6* expression levels were elevated in mD4KO and aD4KO mice on a HCLP diet, but significantly reduced under LCHP feeding. These findings

suggest that a high carbohydrate intake may contribute to unfavorable metabolic changes in skeletal muscle and adipose tissue, while carbohydrate restriction may attenuate these effects.

These results indicate that *Tbc1d4*-deficiency influences the expression of genes involved in lipid metabolism in peripheral tissues in response to macronutrient composition. Under LCHP feeding, reduced *Elovl6* expression levels suggest that carbohydrate restriction may improve insulin sensitivity in states of metabolic dysfunction, potentially lowering the risk of T2D.

4.5 Hepatic FASN abundance is influenced by a high-fat diet in Tbc1d4 deficiency

Reduced hepatic FASN abundance in response to high-fat diets suggests that dietary fat content plays a central role in regulating enzymes responsible for lipid synthesis in *Tbc1d4*-deficient mice. FASN is a pivotal enzyme in de novo lipogenesis, catalyzing the synthesis of long-chain fatty acids such as palmitate. Inhibition of *Fasn* has previously been shown to prevent hepatic steatosis and fibrosis [94].

In the present study, FASN protein abundance was consistently lower across all genotypes under both HCLP and LCHP diets compared to the control diet. The highest abundance of FASN was observed under control feeding conditions, suggesting that the fat content of the diet, rather than the carbohydrate content, is the primary factor suppressing hepatic FASN abundance.

These findings suggest that high-fat diets, irrespective of carbohydrate content or *Tbc1d4* genotype, suppress hepatic FASN abundance, which may contribute to reduced DNL. This finding highlights the impact of dietary fat composition on hepatic lipid metabolism, irrespective of peripheral insulin sensitivity or glucose metabolism.

4.6 Potential link between GLUT4 dysfunction and Hepatic Mlxipl expression in aD4KO mice

Reduced *Mlxipl* expression levels in aD4KO mice fed a LCHP diet suggest a potential association between reduced GLUT4-mediated glucose uptake in adipose tissue and hepatic ChREBP signaling in response to dietary carbohydrates. *Mlxipl* encodes

ChREBP, a transcription factor that is activated by glucose and that has been shown to promote the expression of lipogenic genes, such as *Fasn*, in hepatocytes. ChREBP functions as a central regulator of hepatic metabolic adaptation by coupling carbohydrate availability to lipogenesis [95].

In this study, hepatic *Mlxipl* expression levels were elevated in all *Tbc1d4*-deficient genotypes under HCLP feeding, while expression levels were lowest in aD4KO mice fed a LCHP diet. These findings are somewhat unexpected, as ChREBP has been shown to exert protective effects on hepatic glucose and lipid metabolism in prior studies, as well as on hepatic lipid accumulation in mice [96, 97]. However, it is important to note that previous studies used different mouse models and dietary regimens, and none directly examined *Tbc1d4*-deficiency.

Interestingly, *Mlxipl* expression levels were lowest in aD4KO mice on the LCHP diet, possibly indicating that impaired GLUT4-mediated glucose uptake in adipose tissue influences hepatic ChREBP activity. Supporting this, previous work has shown that ChREBP knockdown in adipose tissue can impair GLUT4 expression and function [82].

Collectively, these findings suggest a genotype- and diet-specific regulation of *Mlxipl* and imply a potential association between adipose GLUT4 dysfunction and hepatic ChREBP signaling in *Tbc1d4*-deficient mice.

4.7 Conclusion and outlook

The present study aimed to further confirm the deleterious effects of a HCLP diet on glucose and lipid metabolism in *Tbc1d4*-deficient mice and to provide additional data that would further support the protective effects of a LCHP diet. This study, with a particular emphasis on the liver, demonstrates that the two diets induce modifications in hepatic glucose and, more markedly, lipid metabolism. A HCLP diet was observed to modulate the gene expression of central enzymes in lipid metabolism, thereby promoting increased lipid accumulation. These deleterious effects could be attenuated when mice were fed a LCHP diet.

Furthermore, alterations in hepatic gene expression or protein abundance are dependent on the tissue in which *Tbc1d4* is knocked out, which serves to confirm the complex interplay between the liver and peripheral insulin-responsive tissues in the regulation of glucose and lipid metabolism. Additionally, these changes appear to be dependent on the macronutrient ratios of the diet fed to these mice.

It is noteworthy that we observed discrepancies in expression levels between D4KO, mD4KO, and aD4KO mice subjected to different diets. We also observed discrepancies between their respective WT or floxed controls under identical dietary conditions. This outcome is not anticipated, as loxP sites alone are not expected to alter gene function. It is important to note, however, that D4KO mice and their WT controls were maintained on an RCS.B6.SJL recombinant congenic background, whereas mD4KO, aD4KO, and their floxed controls were on a pure C57BL/6J background. These disparate genetic backgrounds likely contributed to the observed discrepancies and limit the direct comparability across models. Additionally, variations in the sample size of the animal subjects could further contribute to the observed discrepancies. The sample size ranged from n=6 to 9.

The alterations in lipid and glucose metabolism are not only noticeable at the gene and protein level, but also manifest as changes in hepatic TG levels. The elevated TG levels observed in global D4KO mice fed a HCLP diet indicate that this diet may promote TG accumulation in the liver, thereby potentially contributing to the development and progression of MASLD in *Tbc1d4*-deficiency. These findings are consistent with our observations of enhanced lipid metabolism in knockout mice on a HCLP diet. A LCHP diet was demonstrated to impede TG accumulation in global D4KO

mice, indicating that this dietary regimen may confer protective effects against hepatic lipid accumulation and MASLD. In the light of the findings of Muhammad *et al.* that Greenlanders with diabetes appeared to be protected from liver complications [64], a further investigation into the role of diet and genetic testing in this cohort would be of interest. This would help to elucidate whether diet is one of the protective factors on liver complications in this population.

With regard to individuals who are homozygous for the *p.Arg684Ter* variant, it is possible that the traditional dietary patterns, low in carbohydrates and high in protein and fat, could serve to protect this population from alterations in glucose and lipid metabolism that predispose them to developing T2D and MASLD. While the response to a LCHP diet appears to be individual and possibly genetically determined [98, 99], some individuals may benefit from this dietary intervention. Consequently, a LCHP diet could be utilized as a preventative measure for specific individuals and potentially serve as a therapeutic option for patients with T2D or MASLD.

The objective of this study was to examine the impact of carbohydrate and protein composition on hepatic energy substrate metabolism. As the specific component of the WD that causes deleterious effects on metabolism and the development of metabolic diseases remains unknown, further elucidation of the effects of specific diet components would be of interest. For instance, fructose has been identified as a key factor in DNL and the pathogenesis of MASLD [100, 101]. Moreover, saturated fatty acids have been linked to adverse effects on metabolism and the development of metabolic diseases, whereas polyunsaturated n-3 fatty acids have been shown to exert protective effects [102, 103]. It would be beneficial for future research to gain a deeper understanding of the impact of these specific dietary components on lipid and glucose metabolism in *Tbc1d4*-deficient mice. This would enable the development of a more targeted dietary plan for individuals carrying the homozygous *p.Arg684Ter* variant.

5 References

1. Goyal, R., M. Singhal, and I. Jialal, *Type 2 Diabetes*, in *StatPearls*. 2024, StatPearls Publishing

Copyright © 2024, StatPearls Publishing LLC.: Treasure Island (FL).
2. *Diagnosis and classification of diabetes mellitus.* Diabetes Care, 2010. **33 Suppl 1**(Suppl 1): p. S62-9.
3. Sapra, A. and P. Bhandari, *Diabetes*, in *StatPearls*. 2025, StatPearls Publishing

Copyright © 2025, StatPearls Publishing LLC.: Treasure Island (FL).
4. Kharroubi, A.T. and H.M. Darwish, *Diabetes mellitus: The epidemic of the century.* World J Diabetes, 2015. **6**(6): p. 850-67.
5. . 2021.
6. James, M., et al., *Association Between Metabolic Syndrome and Diabetes Mellitus According to International Diabetic Federation and National Cholesterol Education Program Adult Treatment Panel III Criteria: a Cross-sectional Study.* J Diabetes Metab Disord, 2020. **19**(1): p. 437-443.
7. Hu, F.B., *Globalization of diabetes: the role of diet, lifestyle, and genes.* Diabetes Care, 2011. **34**(6): p. 1249-57.
8. Lu, X., et al., *Type 2 diabetes mellitus in adults: pathogenesis, prevention and therapy.* Signal Transduct Target Ther, 2024. **9**(1): p. 262.
9. Sagastume, D., et al., *The effectiveness of lifestyle interventions on type 2 diabetes and gestational diabetes incidence and cardiometabolic outcomes: A systematic review and meta-analysis of evidence from low- and middle-income countries.* EClinicalMedicine, 2022. **53**: p. 101650.
10. Kreienkamp, R.J., et al., *Genetics of Type 2 Diabetes*, in *Diabetes in America*, J.M. Lawrence, et al., Editors. 2023, National Institute of Diabetes and Digestive and Kidney Diseases (NIDDK): Bethesda (MD).
11. Fenwick, P.H., et al., *Lifestyle genomics and the metabolic syndrome: A review of genetic variants that influence response to diet and exercise interventions.* Crit Rev Food Sci Nutr, 2019. **59**(13): p. 2028-2039.
12. Kotani, K., et al., *GLUT4 glucose transporter deficiency increases hepatic lipid production and peripheral lipid utilization.* J Clin Invest, 2004. **114**(11): p. 1666-75.
13. Fonseca, V.A., *Defining and characterizing the progression of type 2 diabetes.* Diabetes Care, 2009. **32 Suppl 2**(Suppl 2): p. S151-6.
14. Smith, R.L., et al., *Metabolic Flexibility as an Adaptation to Energy Resources and Requirements in Health and Disease.* Endocr Rev, 2018. **39**(4): p. 489-517.
15. Lee, S.H., S.Y. Park, and C.S. Choi, *Insulin Resistance: From Mechanisms to Therapeutic Strategies.* Diabetes Metab J, 2022. **46**(1): p. 15-37.
16. Colosimo, S., et al., *Insulin resistance and metabolic flexibility as drivers of liver and cardiac disease in T2DM.* Diabetes Res Clin Pract, 2023. **206**: p. 111016.
17. da Silva Rosa, S.C., et al., *Mechanisms of muscle insulin resistance and the cross-talk with liver and adipose tissue.* Physiol Rep, 2020. **8**(19): p. e14607.
18. Abdul-Ghani, M.A. and R.A. DeFronzo, *Pathogenesis of insulin resistance in skeletal muscle.* J Biomed Biotechnol, 2010. **2010**: p. 476279.
19. Goodpaster, B.H. and L.M. Sparks, *Metabolic Flexibility in Health and Disease.* Cell Metab, 2017. **25**(5): p. 1027-1036.
20. Li, M., et al., *Trends in insulin resistance: insights into mechanisms and therapeutic strategy.* Signal Transduct Target Ther, 2022. **7**(1): p. 216.
21. *EASL-EASD-EASO Clinical Practice Guidelines on the management of metabolic dysfunction-associated steatotic liver disease (MASLD).* J Hepatol, 2024. **81**(3): p. 492-542.
22. Gastaldelli, A. and K. Cusi, *From NASH to diabetes and from diabetes to NASH: Mechanisms and treatment options.* JHEP Rep, 2019. **1**(4): p. 312-328.

23. Nogueira, J.P. and K. Cusi, *Role of Insulin Resistance in the Development of Nonalcoholic Fatty Liver Disease in People With Type 2 Diabetes: From Bench to Patient Care.* Diabetes Spectr, 2024. **37**(1): p. 20-28.
24. Basaranoglu, M., G. Basaranoglu, and E. Bugianesi, *Carbohydrate intake and nonalcoholic fatty liver disease: fructose as a weapon of mass destruction.* Hepatobiliary Surg Nutr, 2015. **4**(2): p. 109-16.
25. Yu, S., et al., *The Contribution of Dietary Fructose to Non-alcoholic Fatty Liver Disease.* Front Pharmacol, 2021. **12**: p. 783393.
26. Kopp, W., *How Western Diet And Lifestyle Drive The Pandemic Of Obesity And Civilization Diseases.* Diabetes Metab Syndr Obes, 2019. **12**: p. 2221-2236.
27. García-Montero, C., et al., *Nutritional Components in Western Diet Versus Mediterranean Diet at the Gut Microbiota-Immune System Interplay. Implications for Health and Disease.* Nutrients, 2021. **13**(2).
28. Biobaku, F., et al., *Macronutrient-Mediated Inflammation and Oxidative Stress: Relevance to Insulin Resistance, Obesity, and Atherogenesis.* J Clin Endocrinol Metab, 2019. **104**(12): p. 6118-6128.
29. Rakhra, V., et al., *Obesity and the Western Diet: How We Got Here.* Mo Med, 2020. **117**(6): p. 536-538.
30. Hosseini, F., et al., *Dietary carbohydrate and the risk of type 2 diabetes: an updated systematic review and dose-response meta-analysis of prospective cohort studies.* Sci Rep, 2022. **12**(1): p. 2491.
31. Espinosa-Salas, S. and M. Gonzalez-Arias, *Nutrition: Macronutrient Intake, Imbalances, and Interventions*, in *StatPearls*. 2025, StatPearls Publishing

Copyright © 2025, StatPearls Publishing LLC.: Treasure Island (FL).

32. Dashti, H.M., T.C. Mathew, and N.S. Al-Zaid, *Efficacy of Low-Carbohydrate Ketogenic Diet in the Treatment of Type 2 Diabetes.* Med Princ Pract, 2021. **30**(3): p. 223-235.
33. O'Dea, K., *Marked improvement in carbohydrate and lipid metabolism in diabetic Australian aborigines after temporary reversion to traditional lifestyle.* Diabetes, 1984. **33**(6): p. 596-603.
34. Pearson, E.R., *Dissecting the Etiology of Type 2 Diabetes in the Pima Indian Population.* Diabetes, 2015. **64**(12): p. 3993-5.
35. Fumagalli, M., et al., *Greenlandic Inuit show genetic signatures of diet and climate adaptation.* Science, 2015. **349**(6254): p. 1343-7.
36. Looker, H.C., et al., *Diagnostic criteria and etiopathogenesis of type 2 diabetes and its complications: Lessons from the Pima Indians.* Presse Med, 2023. **52**(1): p. 104176.
37. Nakrani, M.N., R.H. Wineland, and F. Anjum, *Physiology, Glucose Metabolism*, in *StatPearls*. 2024, StatPearls Publishing

Copyright © 2024, StatPearls Publishing LLC.: Treasure Island (FL).

38. Han, H.S., et al., *Regulation of glucose metabolism from a liver-centric perspective.* Exp Mol Med, 2016. **48**(3): p. e218.
39. Saltiel, A.R. and C.R. Kahn, *Insulin signalling and the regulation of glucose and lipid metabolism.* Nature, 2001. **414**(6865): p. 799-806.
40. Santoleri, D.T., Paul M. , *Resolving the Paradox of Hepatic Insulin Resistance.* cmgh, 2019. **7**(2): p. p447-456.
41. Espelage, L., H. Al-Hasani, and A. Chadt, *RabGAPs in skeletal muscle function and exercise.* J Mol Endocrinol, 2020. **64**(1): p. R1-r19.
42. Sano, H., et al., *Insulin-stimulated phosphorylation of a Rab GTPase-activating protein regulates GLUT4 translocation.* J Biol Chem, 2003. **278**(17): p. 14599-602.
43. Luo, L. and M. Liu, *Adipose tissue in control of metabolism.* Journal of Endocrinology, 2016. **231**(3): p. R77-R99.
44. Chadt, A., et al., *"Deletion of both Rab-GTPase–activating proteins TBC1D1 and TBC1D4 in mice eliminates insulin- and AICAR-stimulated glucose transport [corrected].* Diabetes, 2015. **64**(3): p. 746-59.

45. Park, S.Y., et al., *Crystal structures of human TBC1D1 and TBC1D4 (AS160) RabGTPase-activating protein (RabGAP) domains reveal critical elements for GLUT4 translocation.* J Biol Chem, 2011. **286**(20): p. 18130-8.
46. Mafakheri, S., et al., *AKT and AMP-activated protein kinase regulate TBC1D1 through phosphorylation and its interaction with the cytosolic tail of insulin-regulated aminopeptidase IRAP.* J Biol Chem, 2018. **293**(46): p. 17853-17862.
47. Sakamoto, K. and G.D. Holman, *Emerging role for AS160/TBC1D4 and TBC1D1 in the regulation of GLUT4 traffic.* Am J Physiol Endocrinol Metab, 2008. **295**(1): p. E29-37.
48. Stöckli, J., et al., *The RabGAP TBC1D1 plays a central role in exercise-regulated glucose metabolism in skeletal muscle.* Diabetes, 2015. **64**(6): p. 1914-22.
49. Wang, H.Y., et al., *AS160 deficiency causes whole-body insulin resistance via composite effects in multiple tissues.* Biochem J, 2013. **449**(2): p. 479-89.
50. Zhou, Z., et al., *Rab28 is a TBC1D1/TBC1D4 substrate involved in GLUT4 trafficking.* FEBS Lett, 2017. **591**(1): p. 88-96.
51. Benninghoff, T., et al., *The RabGAPs TBC1D1 and TBC1D4 Control Uptake of Long-Chain Fatty Acids Into Skeletal Muscle via Fatty Acid Transporter SLC27A4/FATP4.* Diabetes, 2020. **69**(11): p. 2281-2293.
52. Mikłosz, A., et al., *The Effects of AS160 Modulation on Fatty Acid Transporters Expression and Lipid Profile in L6 Myotubes.* Cell Physiol Biochem, 2016. **38**(1): p. 267-82.
53. Samovski, D., et al., *Insulin and AMPK regulate FA translocase/CD36 plasma membrane recruitment in cardiomyocytes via Rab GAP AS160 and Rab8a Rab GTPase.* J Lipid Res, 2012. **53**(4): p. 709-17.
54. Stone, S., et al., *TBC1D1 is a candidate for a severe obesity gene and evidence for a gene/gene interaction in obesity predisposition.* Hum Mol Genet, 2006. **15**(18): p. 2709-20.
55. Dash, S., et al., *A truncation mutation in TBC1D4 in a family with acanthosis nigricans and postprandial hyperinsulinemia.* Proc Natl Acad Sci U S A, 2009. **106**(23): p. 9350-5.
56. Moltke, I., et al., *A common Greenlandic TBC1D4 variant confers muscle insulin resistance and type 2 diabetes.* Nature, 2014. **512**(7513): p. 190-3.
57. Kristensen, J.M., et al., *Skeletal muscle from TBC1D4 p.Arg684Ter variant carriers is severely insulin resistant but exhibits normal metabolic responses during exercise.* Nat Metab, 2024. **6**(12): p. 2254-2266.
58. Overvad, M., et al., *The effect of diabetes and the common diabetogenic TBC1D4 p.Arg684Ter variant on cardiovascular risk in Inuit in Greenland.* Sci Rep, 2020. **10**(1): p. 22081.
59. Bjerregaard, P., et al., *Inuit health in Greenland: a population survey of life style and disease in Greenland and among Inuit living in Denmark.* Int J Circumpolar Health, 2003. **62 Suppl 1**: p. 3-79.
60. Lewis, J.I., et al., *The effect of traditional diet on glucose homoeostasis in carriers and non-carriers of a common TBC1D4 variant in Greenlandic Inuit: a randomised crossover study.* Br J Nutr, 2023. **130**(11): p. 1871-1884.
61. Xie, B., et al., *The Inactivation of RabGAP Function of AS160 Promotes Lysosomal Degradation of GLUT4 and Causes Postprandial Hyperglycemia and Hyperinsulinemia.* Diabetes, 2016. **65**(11): p. 3327-3340.
62. Scheel, A.K., *Metabolic flexibility in early diabetes development*. 2024 Heinrich Heine University
63. Springer, C., et al., *Depletion of TBC1D4 Improves the Metabolic Exercise Response by Overcoming Genetically Induced Peripheral Insulin Resistance.* Diabetes, 2024. **73**(7): p. 1058-1071.
64. Muhammad, A.G., et al., *Non-alcoholic fatty liver disease in patients with type 2 diabetes in Greenland: a register-based cross-sectional study.* Int J Circumpolar Health, 2022. **81**(1): p. 2065755.
65. Smith, P.K., et al., *Measurement of protein using bicinchoninic acid.* Anal Biochem, 1985. **150**(1): p. 76-85.

66. Sharon, R. and D. Naor, *The isolation of immunogenic molecular entities from immunogenic and nonimmunogenic tumor homogenates by sodium dodecyl sulfate polyacrylamide gel electrophoresis (SDS-PAGE).* Cancer Immunol Immunother, 1984. **18**(3): p. 203-8.
67. Fletcher, J.A., et al., *Impaired ketogenesis and increased acetyl-CoA oxidation promote hyperglycemia in human fatty liver.* JCI Insight, 2019. **5**(11).
68. Wang, Y., et al., *Acetyl-CoA Carboxylases and Diseases.* Front Oncol, 2022. **12**: p. 836058.
69. Li, L.Y., et al., *Interplay and cooperation between SREBF1 and master transcription factors regulate lipid metabolism and tumor-promoting pathways in squamous cancer.* Nat Commun, 2021. **12**(1): p. 4362.
70. Schroeder, B., et al., *Fatty acid synthase (FASN) regulates the mitochondrial priming of cancer cells.* Cell Death Dis, 2021. **12**(11): p. 977.
71. Sun, Q., et al., *SCD1 is the critical signaling hub to mediate metabolic diseases: Mechanism and the development of its inhibitors.* Biomed Pharmacother, 2024. **170**: p. 115586.
72. Li, S.W., et al., *Polymorphisms in FADS1 and FADS2 alter plasma fatty acids and desaturase levels in type 2 diabetic patients with coronary artery disease.* J Transl Med, 2016. **14**: p. 79.
73. Zhao, H., et al., *Elovl6 Deficiency Improves Glycemic Control in Diabetic db/db Mice by Expanding β-Cell Mass and Increasing Insulin Secretory Capacity.* Diabetes, 2017. **66**(7): p. 1833-1846.
74. Moffat, C., et al., *Acyl-CoA thioesterase-2 facilitates mitochondrial fatty acid oxidation in the liver.* J Lipid Res, 2014. **55**(12): p. 2458-70.
75. Choi, J., et al., *Carnitine palmitoyltransferase 1 facilitates fatty acid oxidation in a non-cell-autonomous manner.* Cell Rep, 2024. **43**(12): p. 115006.
76. Bougarne, N., et al., *Molecular Actions of PPARα in Lipid Metabolism and Inflammation.* Endocr Rev, 2018. **39**(5): p. 760-802.
77. Younossi, Z.M., M. Kalligeros, and L. Henry, *Epidemiology of metabolic dysfunction-associated steatotic liver disease.* Clin Mol Hepatol, 2025. **31**(Suppl): p. S32-s50.
78. Li, Y., et al., *Updated mechanisms of MASLD pathogenesis.* Lipids Health Dis, 2024. **23**(1): p. 117.
79. Zhu, X.R., et al., *Identification of phosphoenolpyruvate carboxykinase 1 as a potential therapeutic target for pancreatic cancer.* Cell Death Dis, 2021. **12**(10): p. 918.
80. Marchelek-Mysliwiec, M., et al., *The Role of Forkhead Box O in Pathogenesis and Therapy of Diabetes Mellitus.* Int J Mol Sci, 2022. **23**(19).
81. de Zeeuw, P., et al., *The gluconeogenesis enzyme PCK2 has a non-enzymatic role in proteostasis in endothelial cells.* Commun Biol, 2024. **7**(1): p. 618.
82. Agius, L., S.S. Chachra, and B.E. Ford, *The Protective Role of the Carbohydrate Response Element Binding Protein in the Liver: The Metabolite Perspective.* Front Endocrinol (Lausanne), 2020. **11**: p. 594041.
83. Fernandes, L.M., et al., *Malic Enzyme 1 (ME1) is pro-oncogenic in Apc(Min/+) mice.* Sci Rep, 2018. **8**(1): p. 14268.
84. Yuan, M., et al., *Targeting PKLR in liver diseases.* Trends Endocrinol Metab, 2025.
85. Mandard, S., et al., *Glycogen synthase 2 is a novel target gene of peroxisome proliferator-activated receptors.* Cell Mol Life Sci, 2007. **64**(9): p. 1145-57.
86. Kitada, M., et al., *Sirtuins as possible drug targets in type 2 diabetes.* Curr Drug Targets, 2013. **14**(6): p. 622-36.
87. Tamura, Y.O., et al., *Selective Acetyl-CoA Carboxylase 1 Inhibitor Improves Hepatic Steatosis and Hepatic Fibrosis in a Preclinical Nonalcoholic Steatohepatitis Model.* J Pharmacol Exp Ther, 2021. **379**(3): p. 280-289.
88. Al-Dwairi, A., et al., *Cytosolic malic enzyme 1 (ME1) mediates high fat diet-induced adiposity, endocrine profile, and gastrointestinal tract proliferation-associated biomarkers in male mice.* PLoS One, 2012. **7**(10): p. e46716.

89. Lin, Y., Y. Wang, and P.F. Li, *PPARα: An emerging target of metabolic syndrome, neurodegenerative and cardiovascular diseases.* Front Endocrinol (Lausanne), 2022. **13**: p. 1074911.
90. Montagner, A., et al., *Liver PPARα is crucial for whole-body fatty acid homeostasis and is protective against NAFLD.* Gut, 2016. **65**(7): p. 1202-14.
91. Athinarayanan, S.J., *Role of FADS1 in Nonalcoholic Fatty Liver Disease (NAFLD)*, in *Purdue University*. 2017.
92. Chella Krishnan, K., et al., *Liver Pyruvate Kinase Promotes NAFLD/NASH in Both Mice and Humans in a Sex-Specific Manner.* Cell Mol Gastroenterol Hepatol, 2021. **11**(2): p. 389-406.
93. Matsuzaka, T., et al., *Crucial role of a long-chain fatty acid elongase, Elovl6, in obesity-induced insulin resistance.* Nat Med, 2007. **13**(10): p. 1193-202.
94. O'Farrell, M., et al., *FASN inhibition targets multiple drivers of NASH by reducing steatosis, inflammation and fibrosis in preclinical models.* Sci Rep, 2022. **12**(1): p. 15661.
95. Iizuka, K., K. Takao, and D. Yabe, *ChREBP-Mediated Regulation of Lipid Metabolism: Involvement of the Gut Microbiota, Liver, and Adipose Tissue.* Front Endocrinol (Lausanne), 2020. **11**: p. 587189.
96. Jois, T., et al., *Deletion of hepatic carbohydrate response element binding protein (ChREBP) impairs glucose homeostasis and hepatic insulin sensitivity in mice.* Mol Metab, 2017. **6**(11): p. 1381-1394.
97. Iizuka, K., B. Miller, and K. Uyeda, *Deficiency of carbohydrate-activated transcription factor ChREBP prevents obesity and improves plasma glucose control in leptin-deficient (ob/ob) mice.* Am J Physiol Endocrinol Metab, 2006. **291**(2): p. E358-64.
98. Aberle, J., et al., *Genetic variation may influence obesity only under conditions of diet: analysis of three candidate genes.* Mol Genet Metab, 2008. **95**(3): p. 188-91.
99. de Luis, D.A., et al., *Effects of a High-Protein/Low-Carbohydrate Diet versus a Standard Hypocaloric Diet on Weight and Cardiovascular Risk Factors: Role of a Genetic Variation in the rs9939609 FTO Gene Variant.* J Nutrigenet Nutrigenomics, 2015. **8**(3): p. 128-36.
100. Tao, R., et al., *Fructose and follistatin potentiate acute MASLD during complete hepatic insulin resistance.* Nat Commun, 2025. **16**(1): p. 11595.
101. Wang, L., et al., *New light on ω-3 polyunsaturated fatty acids and diabetes debate: a population pharmacokinetic-pharmacodynamic modelling and intake threshold study.* Nutr Diabetes, 2024. **14**(1): p. 8.
102. Rosqvist, F., et al., *Overeating Saturated Fat Promotes Fatty Liver and Ceramides Compared With Polyunsaturated Fat: A Randomized Trial.* J Clin Endocrinol Metab, 2019. **104**(12): p. 6207-6219.
103. Risérus, U. and M. Fridén, *Cardiometabolic benefits of replacing saturated fatty acids with unsaturated fatty acids.* Curr Opin Clin Nutr Metab Care, 2026. **29**(2): p. 131-135.

6 Appendix

6.1 List of tables

Table 1: Mouse strains 15
Table 2: Composition of mouse diets 15
Table 3: Chemicals 16
Table 4: Buffers and solutions 17
Table 5: Reactions kits 17
Table 6: Molecular weight size markers 18
Table 7: Antibodies 18
Table 8: SYBR-Green Primers 19
Table 9: Devices 20
Table 10: Software 20
Table 11: Composition of the SDS gel 24

6.2 List of figures

Figure 1: Progression and prevalence of MASLD. 4
Figure 2: Involvement of RabGAPs in glucose and fatty acid uptake into skeletal/ myocardial muscle. 9
Figure 3: Impact of dietary macronutrient ratios on postprandial glycemia of *Tbc1d4*-deficient mice. 12
Figure 4: Impact of different macronutrient ratios on fasted plasma ketone bodies in mice with global (D4KO), skeletal muscle-specific (mD4KO) or adipocyte-specific (aD4KO) Tbc1d4-deficiency. 13
Figure 5: Gene expression levels of *Acc1* in the liver of global and tissue-specific D4KO mice. 28
Figure 6: Gene expression levels of *Srebf1* and *Srebf2* in the liver of global and tissue-specific-D4KO mice. 29
Figure 7: Protein abundance of FASN in the liver of global and tissue-specific D4KO mice. 30
Figure 8: Gene expression levels of *Scd1*, *Fads1*, and *Elovl6* in the liver of global and tissue-specific-D4KO mice. 32
Figure 9: Gene expression levels of *Acot2*, *Cpt1*, *Cpt2*, and *Ppara* in the liver of global and tissue-specific-D4KO mice. 34
Figure 10: Glycerol and triglyceride levels in the liver of global D4KO. 35
Figure 11: Gene expression levels of *Pck1* and *FoxO1* in the liver of global and tissue-specific-D4KO mice. 37
Figure 12: Protein abundance of PCK1 and PCK2 in the liver of global and tissue-specific-D4KO mice. 38
Figure 13: Gene expression levels of *Mlxipl*, *Me1*, and *Pklr* in the liver of global and tissue-specific-D4KO mice. 40
Figure 14: Protein abundance of GYS2 in the liver of global and tissue-specific-D4KO mice. 41
Abbildung 15: Gene expression levels of *Sirt1* and *Tbc1d1* in the liver of global and tissue-specific-D4KO mice. 42

Danksagung

In erster Linie möchte ich mich ganz besonders bei PD Dr. Alexandra Chadt bedanken. Zunächst einmal für die Überlassung dieses spannenden Themas. Vor allem aber möchte ich Dir für die exzellente Betreuung danken und dass ich mich bei Fragen oder Problemen jederzeit an Dich wenden konnte. Ich danke Dir für die große Unterstützung während der gesamten Promotionszeit und Deine wertvollen Beiträge und Anregungen, die zu dem Gelingen dieser Arbeit maßgeblich beigetragen haben. Ich habe in dieser Zeit sowohl persönlich als auch fachlich viel gelernt.

Ich bedanke mich zudem herzlichst bei Prof. Dr. Maria Grandoch für die Übernahme des Zweitgutachtens, dem Interesse an meiner Arbeit und den hilfreichen Anregungen im Rahmen des Graduiertenkollegs.

Ein großer Dank gilt Prof. Dr. Hadi Al-Hasani, für die Möglichkeit, meine Doktorarbeit am Institut für Klinische Biochemie und Pathobiochemie des Deutschen Diabetes Zentrums und im Rahmen des Graduiertenkollegs 2576 „vivid“ absolvieren zu dürfen.

Mein tiefer Dank gilt Dr. Anna K. Scheel, die mir die gesamte Zeit über zur Seite gestanden hat. Ich danke Dir für die geduldige Einarbeitung in die mir anfangs noch fremde Laborarbeit und für Deine stetige Bereitschaft Dein Wissen, Deine Erfahrungen und Deine Anregungen mit mir zu teilen. Vielen Dank, dass Du jederzeit für mich da warst und Deine Tür bei Fragen und Problemen immer offenstand. Ich schätze mich sehr glücklich von Dir gelernt haben zu dürfen.

Darüber hinaus möchte ich mich bei allen Kolleg:innen des Deutschen Diabetes Zentrums bedanken, für die außerordentliche Hilfsbereitschaft und Unterstützung, wenn mal etwas nicht geklappt hat.

Zuletzt möchte ich mich bei meinen Freunden und meiner Familie bedanken, die bei Verzweiflung immer ein offenes Ohr hatten und mich unterstützt und aufgemuntert haben. Ein besonderer Dank gilt meiner Schwester Dr. Pia Marlene Förster, die mir in jeder Lebenslage zur Seite steht. Auch während der Promotionszeit hattest Du immer einen guten Rat und konntest mich an deiner Erfahrung Teil haben lassen. Die gemeinsame Zeit am Deutschen Diabetes Zentrum war für mich sehr besonders. Ich weiß, dass ich immer auf Dich zählen kann. Mein wohl größter Dank gilt jedoch meinen

Eltern, die mich schon mein ganzes Leben lang bei allem, was ich mir vornehme, unterstützen. Ohne Euch wäre nichts von alledem möglich gewesen.